



A taxonomic conundrum: Characterizing a cryptic radiation of Asian gracile skinks (Squamata: Scincidae: *Riopa*) in Myanmar

Elyse S. Freitas^{a,*}, Aryeh H. Miller^b, R. Graham Reynolds^b, Cameron D. Siler^a

^a Department of Biology and Sam Noble Oklahoma Museum of Natural History, University of Oklahoma, Norman, OK 73072-7029, USA

^b Department of Biology, University of North Carolina, Asheville, Asheville, NC 28804, USA



ARTICLE INFO

Keywords:
 bModelTest
 Bayesian Phylogenetics and Phylogeography (BPP)
 Cryptic species
 Principal components analysis
 Non-ecological diversification
 Species delimitation

ABSTRACT

Recognizing species-level diversity is important for studying evolutionary patterns across biological disciplines and is critical for conservation efforts. However, challenges remain in delimiting species-level diversity, especially in cryptic radiations where species are genetically divergent but show little morphological differentiation. Using multilocus molecular data, phylogenetic analyses, species delimitation analyses, and morphological data, we examine lineage diversification in a cryptic radiation of *Riopa* skinks in Myanmar. Four species of *Riopa* skinks are currently recognized from Myanmar based on morphological traits, but the boundaries between three of these species, *R. anguina*, *R. lineolata*, and *R. popae*, are not well-defined. We find high levels of genetic diversity within these three species. Our analyses suggest that they may comprise as many as 12 independently evolving lineages, highlighting the extent to which species diversity in the region is underestimated. However, quantitative trait data suggest that these lineages have not differentiated morphologically, possibly indicating that this cryptic radiation represents non-adaptive evolution, although additional data is needed to corroborate this.

1. Introduction

The species is the fundamental taxonomic unit in characterizing biodiversity (de Queiroz, 2005). Diverse biological research fields, including ecology, developmental biology, genetics, and physiology rely on the accurate identification of species-level lineages to analyze and interpret results (Knowlton and Jackson, 1994; Bickford et al., 2007; Bortolus, 2008). Additionally, accurate species identification is crucial for conservation efforts (e.g. Dubois, 2003; Frankham et al., 2012; Seifan et al., 2016; Garnett and Christidis, 2017; Tantipisanuh and Gale, 2018), with organizations such as the IUCN using data on the distribution, ecology, and demography of recognized species for conservation assessments (IUCN-SSC, 2017).

Nevertheless, despite the fundamental nature of the species-level unit in research and conservation, challenges remain in recognizing entities that constitute species. Historically, species were defined based on morphological characteristics (e.g. Linnaeus, 1758); however, with the advent of molecular phylogenetics and phylogenomics, it has become possible to recognize distinct lineages from genetic data alone. Use of molecular data in species identification over the last three decades has indicated that many widespread species actually comprise

multiple genetically divergent morphologically similar cryptic species. Complexes of cryptic species often result from non-ecological speciation, in which diversification is not accompanied by apparent ecological or morphological separation in traditional quantitative traits (Czekanski-Moir and Rundell, 2019). Despite the advance of techniques in molecular-based species identifications, morphology remains a critical component of taxonomy and systematics (Ceríaco et al., 2016); therefore, cryptic radiations present particular challenges for taxonomists because of the lack of criteria for describing species that do not exhibit clear diagnostic phenotypic characters (Barley et al., 2013). As the number of recognized cases of cryptic speciation increases, many people suggest taking an integrative approach towards describing these new species that incorporates morphological, ecological, demographic, and geographic datasets with phylogenetic evidence (e.g. Bauer et al., 2011; Barley et al., 2013; Sukumaran and Knowles, 2017; Singhal et al., 2018; Denham et al., 2019; Duran et al., 2019; Hillis, 2019). However, these integrative approaches, although ideal, are challenging when there is a paucity of genetic samples for lineages or observational data on a group's habits—a situation particularly manifest in tropical scincid lizards.

Lizards in the Family Scincidae (skinks) are a remarkably successful

* Corresponding author at: Department of Biology and Sam Noble Oklahoma Museum of Natural History, University of Oklahoma, 2401 Chautauqua Ave., Norman, OK 73072-7029, USA.

E-mail address: efreitas@ou.edu (E.S. Freitas).

group of vertebrates, comprising more than 1,600 species (Uetz et al., 2019). Found in tropical and temperate regions on all continents except Antarctica, and on most oceanic islands, skinks have evolved a diverse array of ecologies, including terrestrial, fossorial, arboreal, rupicolous, and aquatic and are a major part of the global herpetofauna (Vitt and Caldwell, 2013). Therefore, recognizing species-level diversity is critical to understanding the evolutionary history of these lizards and the role they play in regional ecosystems. However, there has been historical taxonomic confusion and instability for a number of groups (e.g. Linkem et al., 2011; Brandley et al., 2012; Skinner et al., 2013; Erens et al., 2017; Freitas et al., 2019), driven in part by lack of diagnostic morphological characters for genera. Furthermore, within genera, cryptic and non-adaptive diversification appears common, which complicates efforts to quantify species-level diversity of the family—44 of the 94 new scincid species described between 2014 and November 2019 (Uetz et al., 2019) were considered members of formerly recognized widespread species that subsequently were found to be distinct species based on genetic data (Table S1). These taxonomic revisions highlight broadly generalized and highly conserved external morphologies and body plans across species as contributing to difficulties in recognizing taxonomic boundaries.

Despite this high number of taxonomic revisions over the years, it is likely that underestimated levels of cryptic diversity still exist across the family Scincidae, particularly within poorly studied regions of the globe. Previous phylogenetic explorations of Asian Gracile Skinks (genus *Riopa*) from South and Southeast Asia have suggested that the genus harbors substantial genetic diversity beyond what has been formally recognized taxonomically (Freitas et al., 2019), and we report on this unrecognized diversity here. The genus *Riopa* comprises nine recognized species from Bangladesh, India, Maldives, Myanmar, Nepal, Pakistan, and Sri Lanka (Uetz et al., 2019). Members of the genus are semifossorial with small, gracile, and elongate bodies, found in or among rotting logs, loose soil, leaf litter and rocks in dry-semi-dry forest, grassland, and urban habitats across their range (Das, 2010; Vyas, 2014; Bhattacharai et al., 2018; Prasad et al., 2018), although little is known about their natural history in Myanmar (Das, 2010). Long a source of taxonomic confusion due to their lack of diagnostic characters (reviewed in Freitas et al., 2019), *Riopa* recently has been the subject of several revisionary studies which have attempted to elucidate species-level relationships within the genus (Datta-Roy et al., 2014; Freitas et al., 2019). Currently, there are four species of *Riopa* recognized from Myanmar: *R. albopunctata* Gray 1846, *R. anguina* Theobald 1868, *R. lineolata* Stoliczka 1870, and *R. popae* Shreve 1940. Of these, *R. lineolata* and *R. popae* are endemic; *R. albopunctata* was described originally from India but is widespread across southern Asia and is recognized to occur in both countries (Manthey and Grossman, 1997), and *R. anguina*, described originally from Myanmar, also occurs in localities in southwestern Thailand in Prachuap Khiri Khan and Chumphon Provinces (Nabhitabhata et al., 2000; Chan-ard et al., 2015). Historically, the four species from Myanmar have been diagnosed by variation in mensural and meristic characters, including relative limb lengths, midbody scale row count, and coloration (Theobald, 1876; Stoliczka, 1870; Shreve, 1940; Das, 2010; Geissler et al., 2012; Freitas et al., 2019). However, the considerable overlap in these characters between taxa have made recognizing species boundaries difficult (Jayaram, 1949; Vyas, 2001, 2010; Seetharamaraju et al., 2009; Srinivasulu and Seetharamaraju, 2010).

Myanmar is located in Southeast Asia, bordered by India and Bangladesh in the northwest, the Bay of Bengal and the Andaman Sea in the southwest, China and Laos in the northeast, and Thailand in the southeast (Fig. 1). The country is diverse ecologically, varying in habitat type and abiotic factors such as elevation, temperature and precipitation (Fig. 2). Although Myanmar and the surrounding region were not initially identified as a biodiversity hotspot (Myers, 1988, 1990), over the past three decades there has been an increase in recognized species-level biodiversity in the region, prompting its classification as

the Indo-Burma Biodiversity Hotspot (Mittermeier et al., 1999; Myers et al., 2000). During the last five years alone, expeditions across Myanmar have discovered large amounts of population- and species-level diversity among major vertebrate groups and has resulted in the description of 65 new species: ten species of amphibian, 17 species of fish, two species of mammal, and 36 species of reptile (Table S2). However, the level of unrecognized and cryptic diversity within scincid lizards in Myanmar remains poorly understood. In this paper, we use multilocus coalescent-based species delimitation methods and multivariate analyses of morphological data to illustrate that species diversity within the genus *Riopa* in Myanmar is greatly underestimated. The results of our study suggest that the genus has undergone significant lineage diversification with little discernable divergence in external morphology. These levels of potential cryptic species diversity affect our understanding of the evolutionary, biogeographic, and ecological patterns of vertebrate diversification within the country.

2. Materials and methods

2.1. Taxon sampling and molecular methods

Ingroup sampling comprised 41 individuals of *Riopa* from central and northern Myanmar (Fig. 1) identified in museum collections as *R. anguina* (18 individuals), *R. bowringii* (three individuals), *R. lineolata* (nine individuals), *R. popae* (five individuals), and *R. sp.* (six individuals) (Table S3). Several samples were obtained from Mount Popa, the type locality of *R. popae*, and Bago and Yangon provinces, the approximate type locality of *R. anguina*; however, we did not obtain samples from the type locality of *R. lineolata*, which is farther south in Mon State (Fig. 1). Outgroup sampling included GenBank sequences for seven members of three closely related genera: *Lygosoma quadrupes*, *Mochlus brevicaudis*, *M. guineensis*, *M. sundevallii*, *Subdoluseps bowringii*, *S. herberti*, and *S. samajaya*, and one additional species from the genus *Riopa*, *R. albopunctata*, shown previously to be the sister species to Myanmar *Riopa* (Freitas et al., 2019; Table S3). Tissue samples were provided by the California Academy of Science (CAS).

Genomic DNA was extracted from ethanol-preserved liver, muscle, or tail tissue using a high-salt extraction method (Aljanabi and Martinez, 1997) or the Wizard SV® Genomic DNA Purification System (Promega). Extracts were amplified via PCR in 10 μ L reactions following standard protocols (Siler et al., 2011) for three nuclear DNA (nuDNA) loci and three mitochondrial DNA (mtDNA) genes. Nuclear loci comprised brain-derived neurotrophic factor (*BDNF*; 690 base pairs [bp]), RNA fingerprint protein 35 (*R35*; 662 bp), and recombination activating gene 1 (*RAG1*; 891 bp); mtDNA genes comprised NADH dehydrogenase subunit 1 (*ND1*; 966 bp) and subunit 2 (*ND2*; 1032 bp), and 16S ribosomal RNA (16S; 535 bp; Table 1). PCR products were purified by ExoSAP-IT (ThermoFisher Scientific), sequenced with BigDye® Terminator v3.1 sequencing kit (ThermoFisher Scientific) and cleaned using ethanol precipitation. We sent sequencing products to Eurofins Genomics in Louisville, Kentucky or the Genomic Sciences Laboratory at North Carolina State University for visualization. All novel sequences were deposited in GenBank (Table S3).

2.2. Sequence alignment and phylogenetic analyses

Raw sequences were imported into Geneious v10.2.4 (Biomatters, Ltd.), assembled into contigs, and checked for quality. All nuDNA contigs were examined for miscalled heterozygous sites. Once we were satisfied with data quality, we trimmed the primer binding sites from both ends of each contig and aligned contigs using MUSCLE (Edgar, 2004) in Geneious with default settings. Alignments were checked by eye for misplaced indels and, for all coding genes (all genes except 16S), erroneous internal stop codons.

We ran preliminary Maximum Likelihood (ML) analyses in RAxML v8.2.12 (Stamatakis, 2014) on each nuDNA gene separately and on the

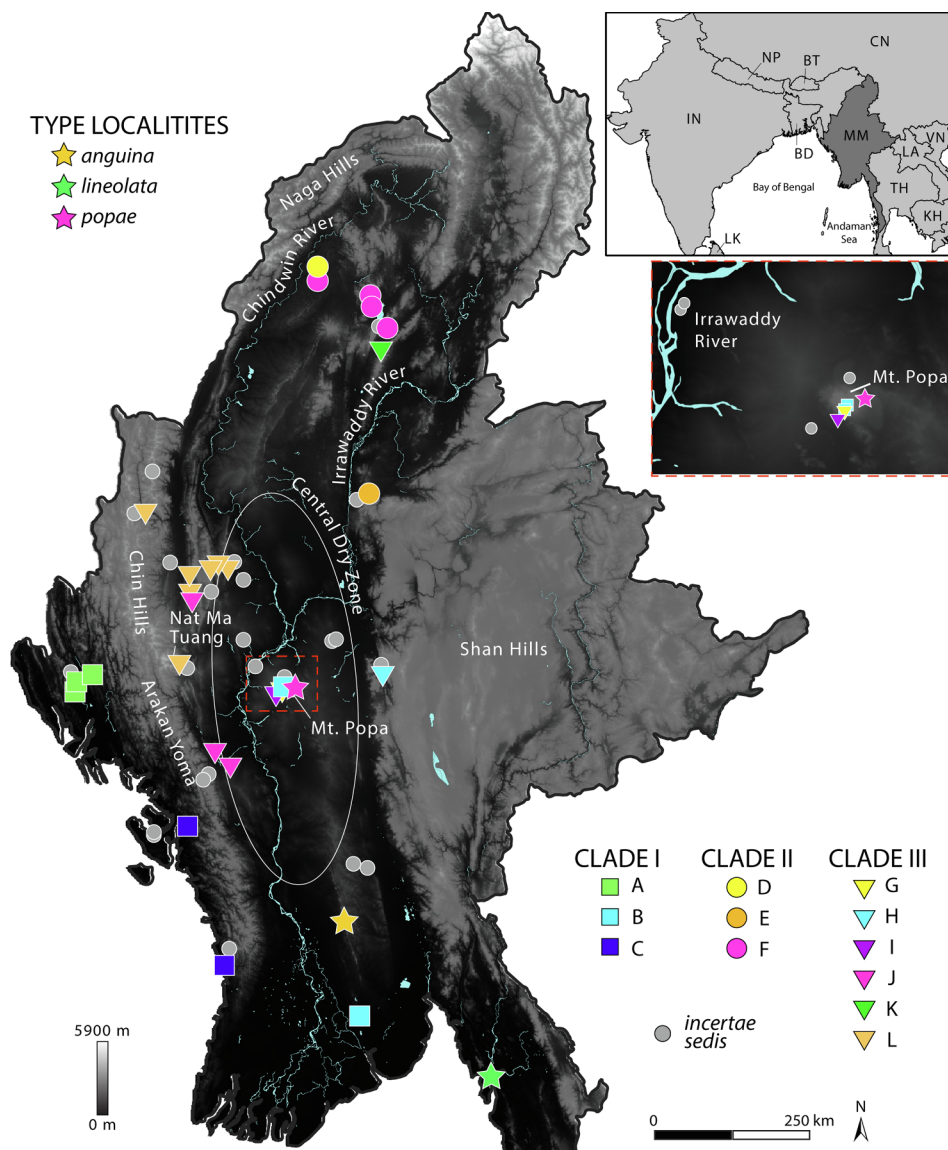


Fig. 1. Map of Myanmar showing localities of specimens and tissues used in this study and the type localities for the three species described from Myanmar. Myanmar is shaded according to elevation, with lighter colors indicating higher elevations. Geographic features mentioned in text are labeled on the map, with the exception of the Central Myanmar Basin, which comprises the low elevation region between the Indo-Myanmar Range in the west (Naga Hills, Chin Hills, Arakan Yoma) and Shan Hills in the east. The lower right inset shows the closeup of sampling around Mount Popa, the type locality of *Riopa popae*. The upper right inset shows the location of Myanmar in South and Southeast Asia, with the countries labeled according to their two letter ISO 3166-1 alpha-2 country codes: BD = Bangladesh, BT = Bhutan, CN = China, IN = India, KH = Cambodia, LA = Laos, LK = Sri Lanka, MM = Myanmar, NP = Nepal, TH = Thailand, VN = Vietnam.

concatenated mtDNA dataset to check for discordance between loci. For ML analyses, *16S* was analyzed as a single partition and nuDNA and mtDNA protein coding genes were partitioned by codon position, and the substitution model GTR + Γ was applied to each partition. Topological support was assessed by 100 bootstrap pseudoreplicates. Results of these analyses showed no incongruence between the mtDNA and nuDNA topologies; therefore, we conducted additional partitioned, phylogenetic analyses on the concatenated nuDNA + mtDNA dataset.

We used BEAST v2.5.1 (Bouckaert et al., 2014) to conduct Bayesian phylogenetic analysis on our concatenated dataset, employing the package bModelTest v1.1.2 (Bouckaert and Drummond, 2017) to calculate the best substitution model for each partition. This approach estimates the phylogeny and the substitution models jointly using a reversible jump Monte Carlo Markov Chain (rjMCMC) algorithm, which allows the chain to analyze substitution models with different numbers of parameters (Bouckaert and Drummond, 2017). We limited our rjMCMC search to models containing different transition-transversion rates for computational efficiency, which includes the Jukes-Cantor model where all rates are equal, the GTR model where all rates are different, and all models where the rate of transitions is different from the rate of transversions—a total of 31 models (Bouckaert and Drummond, 2017). Although bModelTest can search for the best substitution model for each partition, it requires *a priori* selection of the

partitioning scheme. Therefore, like the ML single gene analyses, we partitioned our data by codon position, with the exception of *16S*, which was treated as a single partition. The analysis was run using a relaxed lognormal molecular clock with default priors and a Yule Speciation model with default priors. We applied separate molecular clocks and tree models to the mtDNA and nuDNA. We conducted two runs of 100,000,000 generations each, sampling every 10,000 generations, using the CIPRES Science Gateway (Miller et al., 2010). The results of these two analyses were examined separately and together in Tracer v1.7.1 (Rambaut et al., 2018) and RWTY v1.0.1 (Warren et al., 2017) in R v3.5.0 (R Core Team, 2018) to assess stationarity and convergence, determined by ESS values above 200 for parameters and runs sampling the same regions of tree space in RWTY. The RWTY analyses were run using the command analyze.rwty. Convergence of most parameters occurred after 10,000,000 generations, and so we discarded the first 10% of each run as burnin. We combined the BEAST2 bModelTest analyses in LogCombiner v2.5.1 (Bouckaert et al., 2014), discarding the first 10% of trees in each posterior distribution as burnin (observed as appropriate for cutoff, see above). The output had 18,002 trees in the combined posterior distribution of the final two runs. We used TreeAnnotator v2.5.1 (Bouckaert et al., 2014) to select the maximum clade credibility tree and calculated the posterior probability of each bifurcation.

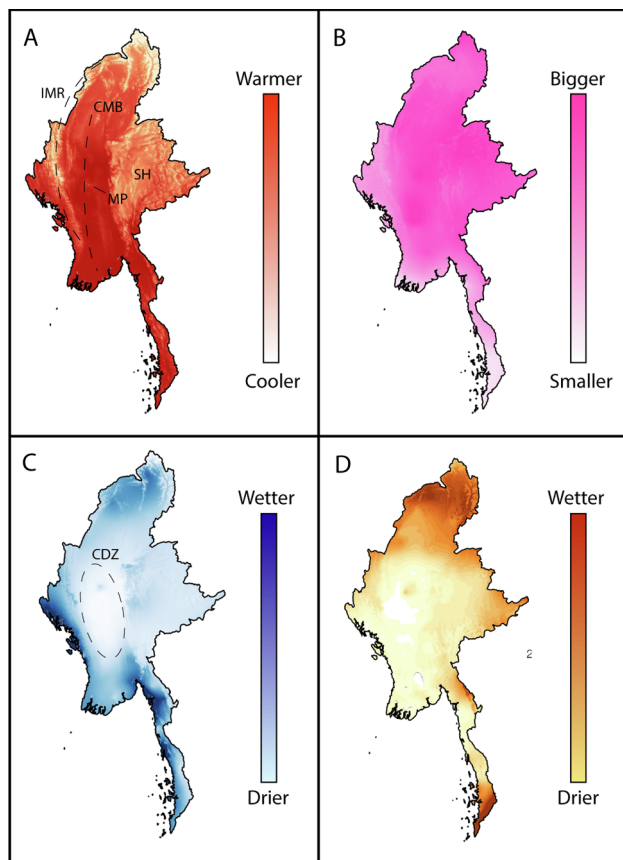


Fig. 2. Maps of Myanmar showing different abiotic gradients: (A) Mean annual temperature; (B) Difference between the mean annual high temperature and the mean annual low temperature; (C) Mean annual precipitation; and (D) Precipitation of the driest month. Abbreviations for geographic features mentioned in text: CMB = Central Myanmar Basin, CDZ = Central Dry Zone, IMR = Indo-Myanmar Range, MP = Mount Popa, SH = Shan Hills.

2.3. Putative lineage identification

The coalescent-based species delimitation program Bayesian Phylogenetics and Phylogeography (BPP), used to delimit species within *Myanmar Riopa* (see below), requires input of putative species-level lineages *a priori* to the analysis. BPP then tests these lineages and determines whether they warrant species-level recognition. Because specimen morphology gives few clues to the species-level identity of each individual, we used barcoding distance thresholds and the Bayesian species delimitation program bGMYC (Reid and Carstens, 2012) to determine lineages objectively within *Myanmar Riopa*. These methods determine groups of samples that can then be used as

hypotheses for species assignment in BPP. We implemented barcoding distance thresholds and bGMYC on our *ND2* ingroup data. As a mtDNA gene, *ND2* has a higher mutation rate than nuDNA loci (Vawter and Brown, 1986), making it useful for detecting structure at shallow nodes in our topology. Additionally, we chose to use *ND2* for species discovery because this gene had the most complete dataset of all our mtDNA markers (Table S3).

The barcoding distance threshold method clusters sequences based on a genetic threshold value determined by the barcoding gap, which is the numerical value not represented in a dataset of pairwise genetic distances, and thus a value that represents the gap between intra- and interspecific genetic diversity (Meyer and Paulay, 2005). Although this approach to lineage identification is purely distance-based and does not account for evolutionary processes, it is useful for identifying monophyletic genetic clusters that serve as *a priori* hypotheses of conspecificity within a set of samples. To implement the barcoding distance threshold method, we first calculated the uncorrected pairwise distance for *ND2* (Table 2, S4) using the command `dist.dna` in the R package `ape` v5.2 (Paradis and Schliep, 2018), and then used these distances to identify the barcoding gap with the command `localMinima` in the R package `Spider` v1.5.0 (Brown et al., 2012) with the barcoding gap corresponding to the lowest local minimum as determined by plotting the distances using the command `plot`. We then determined the number of genetic clusters by setting the barcoding gap as the maximum intraspecific genetic diversity threshold with the command `clust` in `Spider`.

In addition to the barcoding distance threshold method, we used the species delimitation program bGMYC to determine species-level lineages. BGMYC is the Bayesian implementation of GMYC (Pons et al., 2006), which uses the general mixed Yule coalescent model to estimate divergence events on a topology. The program bGMYC goes a step farther, in that it uses the general mixed Yule coalescent model to estimate divergent events on a posterior distribution of topologies, allowing it to incorporate phylogenetic uncertainty into its lineage assignment hypotheses and generate probabilities of conspecificity. Although the program has been used previously in species delimitation studies to identify species-level lineages, it was shown in simulation studies that it overestimates the number of species more often than BPP (Luo et al., 2018); therefore, we used bGMYC instead to identify putative lineages within our *ND2* dataset.

BGMYC requires ultrametric topologies as input and so we generated *ND2* phylogenies with ingroup samples only, using `bModelTest` in BEAST2. We partitioned *ND2* by codon position and used a random local clock. This phylogenetic analysis was run once for 5,000,000 generations sampling every 500 generations and the output was viewed in Tracer to check for convergence, as described above. We used LogCombiner to remove the first 10% of trees as burnin and resample the posterior distribution every 5,000 generations, so that there were 181 trees in our posterior distribution to use as input for bGMYC. We implemented bGMYC in the R package `bGMYC` v1.0.2 (Reid, 2014)

Table 1
The primers, primer sequences, and annealing temperatures used in this study.

Gene	Primer	Sequence (5'-3')	Annealing Temp (°C)	Reference
<i>BDNF</i>	BDNF.F	GACCATCCCTTCCCTKACTATGGTTATTCATACTT	61	Leaché and McGuire (2006)
	BDNF.R	CTATCTCCCTTTAATGGTCAGTGACAAAC		
<i>R35</i>	R35.F	GACTGTGGAYGAYCTGATCAGTGTTGG	55	Fry et al. (2006)
	R35.R	GCCAAAATGAGSGAGAARGCTTCTG		
<i>RAG1</i>	RAG1.R13	TCTGCTGTTAATGGAAATTCAAG	53	Adapted from Groth & Barrowclough, 1999 by unknown
	RAG1.R13.rev	AAAGCAAGGATAGCGACAAGAG		
<i>ND1</i>	16dR	CTACGTGATCTGAGTTAGCAGACCGGAG	53	Leaché and Reeder (2002)
	tMet	TCGGGTATGGGCCARAGCTT		
<i>ND2</i>	ND2_L4437	AAGCTTCTGGGCCATACC	53	Macey et al. (1997)
	ND2_H5730	AGCGAATRGAAGCCCGCTGG		
<i>16S</i>	16Sar-L	CGCCTGTTATCAAAACAT	46	Palumbi (1991)
	16Sbr-H	CCGGCTGAACTCAGATCACGT		

Table 2

The uncorrected pairwise distance for the mitochondrial gene *ND2* for all lineages recovered in barcoding distance thresholds lineage discovery method. The intra-lineage distances are bolded. Distances between lineages within each of the three major clades are highlighted in gray: Clade I = light gray; Clade II = medium gray; Clade III = dark gray.

	Lineage A n=3	Lineage B n=3	Lineage C n=6	Lineage D n=1	Lineage E n=1	Lineage F n=6	Lineage G n=1	Lineage H n=1	Lineage I n=1	Lineage J n=2	Lineage K n=1	Lineage L n=14
Lineage A	0.0–0.3											
Lineage B	10.4– 11.1	0.0–4.7										
Lineage C	9.0–9.6	7.8–9.2	0.5–6.1									
Lineage D	11.1– 11.4	12.4– 13.4	10.8– 12.7	NA								
Lineage E	11.8	12.8– 13.6	11.6– 12.4	8.7	NA							
Lineage F	11.3– 11.7	11.7– 13.1	9.6–12.4	8.5–8.7	9.0–9.2	0.0–0.5						
Lineage G	12.5– 12.8	11.1– 13.1	10.4– 12.8	13.7	13.4	12.5– 12.8	NA					
Lineage H	12.7	12.4– 13.4	11.1– 12.2	12.8	13.1	12.2– 12.5	11.6	NA				
Lineage I	12.2– 12.5	13.3– 14.0	11.3– 12.5	13.4	12.5	12.5– 13.0	12.2	12.7	NA			
Lineage J	10.5– 12.0	10.4– 12.5	10.4– 13.0	11.6– 13.6	10.8– 12.5	10.8– 12.5	11.6– 12.5	10.7– 13.0	9.5–9.6	5.6		
Lineage K	11.4– 12.8	15.4– 15.7	13.3– 14.5	14.2	14.2	14.3– 14.5	13.3	14.5	12.5	11.4– 11.7	NA	
Lineage L	11.1– 12.8	12.2– 14.8	12.0– 14.2	11.9– 13.6	12.0– 13.1	12.7– 13.9	11.7– 12.8	11.4– 12.2	8.7–10.4	7.2–9.3	8.2–10.7	0.0–5.8

using the command `bgmyc.multiphylo`. We ran the MCMC chain for 50,000 generations with a burnin of 25,000 and a thinning interval of 500, which resulted in a total of 9,050 samples in the posterior distribution of the analysis. We used the command plot to visualize the MCMC output and determine if the analysis had converged. Finally, the MCMC samples were analyzed using the command `bgmyc.point` and a threshold value of 0.05, so that individuals or groups of individuals needed a more than 95% chance that they were distinct from other samples to be considered an independent lineage.

Because BPP implements the Jukes-Cantor substitution model, it performs best when samples are separated by less than 10% sequence divergence (Flouri et al., 2018). However, the results of our uncorrected pairwise distance calculation indicated that distances between lineages exceeded 10%. Therefore, we performed barcoding distance threshold and bGMYC on the entire dataset (Fig. 3i, 3ii), as well independently on each of three major clades recovered in phylogenetic analyses (Fig. 3iii, 3iv; Table 3; see results below)

2.4. Species delimitation

To investigate the number of cryptic species within *Myanmar Riopa*, we ran Bayesian species delimitation analyses on our dataset using the program Bayesian Phylogenetics and Phylogeography (BPP) v4.0 (Rannala and Yang, 2003; Yang and Rannala, 2010; Yang, 2015). The program uses rjMCMC to analyze multiple loci under the multispecies coalescent (MSC), and it estimates relative species divergence times and ancestral population sizes. The MSC model implemented in BPP assumes free recombination between loci, no recombination within a given locus, and an absence of gene flow between taxa (Yang, 2015). In a recent simulation study, BPP was shown to outperform other species delimitation methods across different speciation scenarios, generally producing fewer false positives (overestimates of numbers of species) than the other methods (Luo et al., 2018).

We ran the A10 analysis in BPP (species delimitation with a fixed guide tree) to validate the lineages recovered by barcoding threshold distance and bGMYC, basing our guide species tree off the results of our

concatenated phylogenetic analysis (above). To avoid pseudoreplication, we removed *ND2* from our genetic dataset, and we concatenated *ND1* and *16S* so that the mtDNA was treated as a single locus. Therefore, the analysis was run on four loci: *BDNF*, *R35*, *RAG1*, and mtDNA, as well as on the nuDNA dataset only (Table 3). We did not phase our nuDNA for the analysis. We set the parameter locusrate = 1 so that there was rate heterogeneity across loci, and in the combined nuDNA + mtDNA analyses, we used a heredity scaler so that the heredity of nuDNA = 1 and the heredity of mtDNA = 0.25. All other parameters were kept at default values, including the inverse gamma priors θ and τ_0 , with $\theta = (3, 0.002)$ and $\tau_0 = (3, 0.03)$. Each BPP analysis was run twice to check consistency of the performance of the rjMCMC algorithm. Runs were conducted for 20,000 generations, sampled every 10 generations, with a burnin of 8,000 generations.

2.5. Population structure

We used the NeighborNet algorithm (Bryant and Moulton, 2004) as implemented in the program SplitsTree v4.14.8 (Huson and Bryant, 2006) to visualize clade-level diversification and possible reticulating relationships within *Myanmar Riopa*. SplitsTree generates a phylogenetic network, which allows for visualization of all possible evolutionary histories of the samples, including all discordant splits (Huson and Bryant, 2006), giving us a clearer picture of monophyly and genetic differentiation between populations and species. We ran the program on the concatenated mtDNA dataset and on each individual nuDNA gene alignment using HKY-corrected p-distances to generate networks. Support for inferred network splits was assessed with 1,000 bootstrap replicates; splits with bootstrap (bs) values of 70 or higher were considered highly supported (Hillis and Bull, 1993). Lineage assignment was determined based on the results of the BPP analysis of the concatenated nuDNA + mtDNA dataset for 12 putative species.

2.6. Species tree analysis

We conducted species tree analyses on the ingroup taxa using

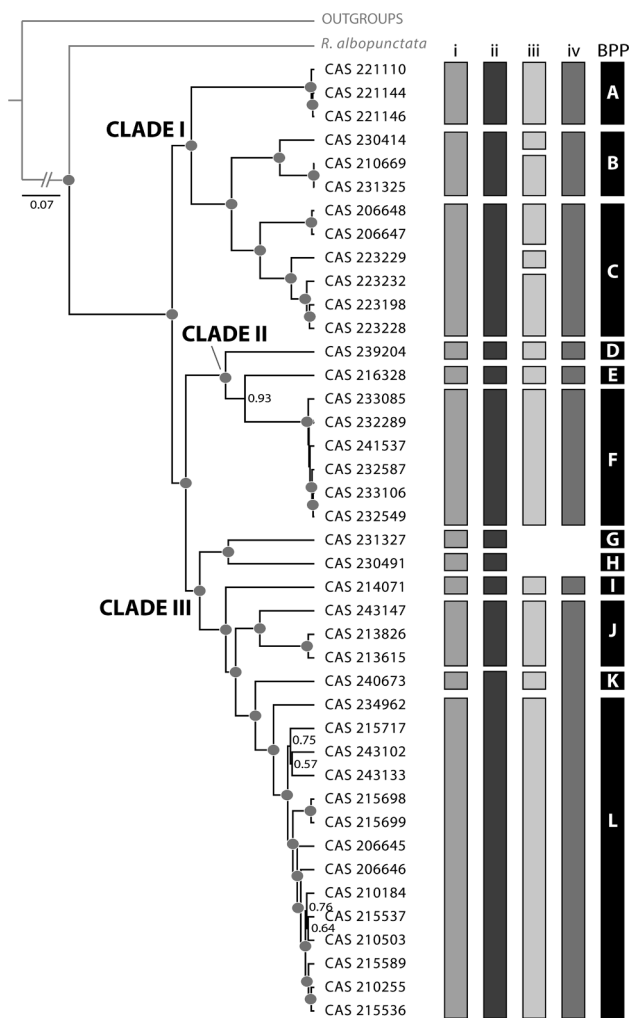


Fig. 3. Phylogeny showing the results of the concatenated bModelTest analysis performed in BEAST2. Gray circles indicate nodes that are highly supported ($pp \geq 0.95$). The scale bar indicates branch lengths in average substitutions over time. The columns to the right of the topology indicate the putative lineages supported by each lineage discovery method: i—barcoding threshold values on the entire dataset; ii—bGMYC on the entire dataset; iii—barcode threshold values on each clade individually; and iv—bGMYC on each clade individually. The final column in black shows lineages supported by the BPP analysis with 12 putative lineages as input.

*BEAST2 v0.15.2 (Ogilvie et al., 2017) in BEAST2. Taxa were designated as a member of a species based on the results of the BPP analysis of the concatenated nuDNA + mtDNA dataset for 12 putative species (Table 3). The results of the previous concatenated bModelTest indicated that several of the nuDNA codon position partitions were uninformative. Therefore, we changed our partitioning strategy for this analysis and partitioned nuDNA by gene instead of by codon position. *ND1* and *ND2* remained partitioned by codon position due to the higher information content of these partitions. We ran bModelTest on the ingroup taxa three times each for 100,000,000 generations, sampling every 10,000 generations, to obtain estimates for the substitution model for each partition. The analysis was run with a random local clock because lineages are all closely related and so we assumed similarity of clock rates with random change across branches (Drummond and Suchard, 2010), and a Yule Speciation model. As in the first bModelTest run, the nuDNA and mtDNA were linked separately so that two trees and two clocks, one each for nuDNA and mtDNA, were estimated. Alpha and beta values on the gamma prior for each clockrate.c parameter were changed to 2.0 and 0.5, respectively, as preliminary runs under default priors produced infinitesimally low values for these parameters and caused the likelihood to approach infinity. All other priors were kept at default values. Substitution model results from this analysis for each partition are shown in Table S5.

We plugged in the substitution models obtained from bModelTest into StarBEAST2 and ran a species tree analysis twice for 100,000,000 generations each, sampling every 10,000 generations. We used a random local clock, and again changed the gamma prior on the clockrates.c parameter to an alpha and beta of 2.0 and 0.5, respectively. We viewed the output in Tracer and RWTY to determine convergence and stationarity, and discarded the first 10% of runs as burnin, leaving 18,002 trees in the posterior distribution.

2.7. Morphological analyses

We examined fluid-preserved specimens of *Riopa* from Myanmar for variation in mensural and meristic characters, selecting characters that have been used in previous skink phylogenetic studies to delimit species (Siler et al., 2010). Our final morphological dataset comprised 86 individuals and contained 14 mensural characters: snout–vent length (SVL), axilla–groin distance (AGD), midbody width (MBW), tail width (TW), tail depth (TD), head length (HL), head width (HW), head depth (HD), eye diameter (ED), eye–nares distance (END), snout length (SNL), internares distance (IND); fore limb length (FLL), and hindlimb length (HLL), and five meristic characters: midbody scale row count (MBSRC), axilla–groin scale row count (AGSRC), paravertebral scale row count (PVSRC), Finger III lamellae (FinIIIILam), and Toe IV lamellae

Table 3

Results of the Bayesian Phylogenetics and Phylogeography (BPP) analyses across all samples and for each clade analyzed separately. Each analysis was run on the complete genetic dataset, excluding *ND2*, which was used in lineage discovery, and on the nuDNA genetic dataset only.

Taxonomic sampling	Lineage identification method	No. putative species	Genes tested in BPP	No. BPP species (pp)
All	barcoding distance thresholds	12	nuDNA, ND1, 16S	12 (1.00)
	bGMYC	11	nuDNA	12 (0.97)
Clade I	barcoding distance thresholds	6	nuDNA, ND1, 16S	11 (1.00)
	bGMYC	3	nuDNA	11 (0.99)
Clade II	barcoding distance thresholds	3	nuDNA, ND1, 16S	6 (0.99)
	bGMYC		nuDNA	6 (0.99)
Clade III	barcoding distance thresholds	4	nuDNA, ND1, 16S	3 (1.00)
	bGMYC	2	nuDNA	3 (1.00)

(ToeIVLam). Additionally, we counted the number of supralabial, infralabial, supraocular, superciliary, loreal, and preocular scales and examined the degree of contact between head scales; however, following the observation that these characters show little to no variation across ingroup samples, they were excluded from subsequent morphological analyses. Measurements were taken by ESF and AHM with digital calipers accurate to 0.01 mm with the exception of SVL and AGD—because older specimens were often fixed with curved bodies, SVL and AGD were measured with a string which was then measured with digital calipers accurate to the 0.01 mm. All scale counts were taken on the right side of the body when possible.

We conducted principal component analyses (PCA) on our mensural and meristic character datasets separately to visualize the distribution of the putative species recovered by BPP in morphospace. We removed individuals with missing data so that the mensural character dataset contained 73 individuals, with 38 of those also included in our phylogenetic analyses, and the meristic character dataset contained 81 individuals, with 45 of those also included in our phylogenetic analyses. Before conducting PCA on the mensural data, we size-corrected individuals to account for the disproportionately large effect of SVL on variance and to address any potential changes in body shape that occur with changes in body size, using the allometric equation: $X_{adj} = \log_{10}(X) - \beta[\log_{10}(SVL) - \log_{10}(SVL_{mean})]$, where X is the original value of the mensural character, X_{adj} is the size-corrected value of the mensural character, SVL_{mean} is the average SVL across all individuals, and β is the linear regression coefficient calculated from $\log_{10}(X)$ against $\log_{10}(SVL)$ (Thorpe, 1975; Leonart et al., 2000). Ideally, we would calculate β for each putative species; however, several hypothesized lineages were represented by a single individual only, making the calculation of β impossible in these instances. Therefore, we calculated one β for each measurement across our dataset, because all individuals in our dataset are members of the same radiation across Myanmar, we feel confident that this did not have a large effect on the results. Prior to conducting the PCAs, we calculated the Z scores for each variable in both the mensural and meristic datasets using the scale function in R to standardize the variance for each variable. We ran each PCA using the command prcomp in R.

3. Results

3.1. DNA sequencing and phylogenetic results

Our molecular dataset comprised 4,776 base pairs for 49 individuals—41 ingroup and eight outgroup samples with a total of 11.2% missing data across the entire concatenated alignment. The majority of missing data was confined to outgroup taxa, with only a few ($n = 7$) ingroup taxa missing locus-specific coverage (Table S3). Our concatenated analyses in bModelTest inferred a well-supported topology (Fig. 3). Similar to the recent higher-level study of *Lygosoma* group skinks (Freitas et al., 2019), we recover a clade of *Riopa* from Myanmar with high support (posterior probability [pp] = 1.0; Fig. 3). Within Myanmar *Riopa*, three major clades are recovered (pp = 1.0 for each; Fig. 3, Clades I–III), each displaying significant intraspecific and well-supported genetic structure. These clades do not correspond to known species—individuals identified to species are not recovered as monophyletic groups (Table S3).

3.2. Cryptic lineage identification and species delimitation

Calculation of the uncorrected p-distances for the *ND2* gene used in barcoding threshold values reveals high levels of genetic diversity between samples, with observed divergences between individuals of up to 15.7% (mean = $10.4 \pm 3.8\%$; Tables 2, S4). Within each of the three major clades (Figs. 1, 3, 6; Clades I–III), the pairwise genetic distances range from 9.2–13.0% (Tables 2, S4). These *ND2* distances were used as input for the lineage barcoding threshold method and resulted in four

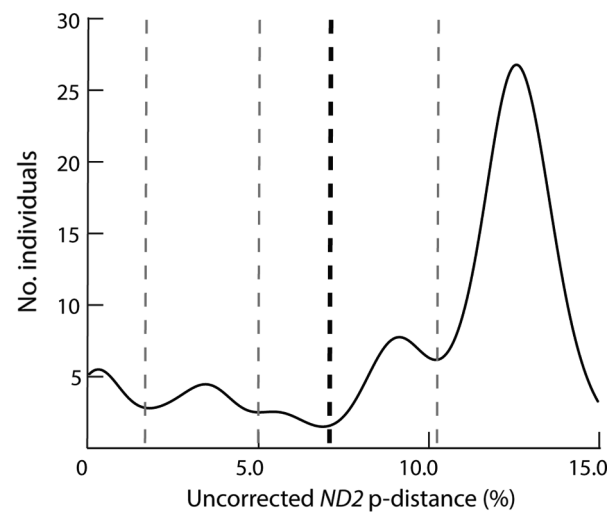


Fig. 4. Graph of the resulting barcoding threshold values for *ND2*. The gray and black dashed lines correspond to minimum values, with the bolded black dashed line at 6.8%, which represents the lowest minimum value. This value (6.8%) was used as the input value for lineage discovery using the barcode threshold method.

potential thresholds at 1.7%, 5.0%, 6.8%, and 10.1%, with 6.8% corresponding to the lowest minimum threshold (Fig. 4). Based on this threshold value, we recovered 12 putative lineages, each comprising 1–14 sampled individuals (Fig. 3; Table 3). Clades I and II each were supported as comprising three lineages and Clade III was supported as comprising six lineages. Comparatively, bGMYC supported 11 putative lineages, with Clades I and II again comprising three lineages, but Clade III instead comprising five lineages (Fig. 3; Table 3). Clade-specific lineage barcoding distance thresholds and bGMYC lineage identification analyses identified six and three putative lineages, respectively for Clade I, three for Clade II, and four and two, respectively for Clade III (Fig. 3; Table 3). These intra-clade analyses excluded lineages G and H from Clade III because these samples were greater than 10% divergent from all other lineages recovered. For within clade barcoding distance thresholds analyses, the threshold values were 2.8% for Clade I, 5.4% for Clade II, and 6.4% for Clade III.

In most cases, BPP analyses identified all input lineages as species with high support (considered to be posterior probabilities of above 0.95; Huelsenbeck and Rannala, 2004; Yang and Rannala, 2010) for both concatenated (nuDNA + mtDNA) and nuDNA only datasets. The exception was poor support (pp = 0.52) observed for four putative lineages within Clade III in analyses of the concatenated dataset however, each of the same four lineages was highly supported (pp = 0.98) in analyses of the nuDNA only dataset (Fig. 3; Table 3).

3.3. Phylogenetic networks

Analysis of genetic structure using SplitsTree revealed that individual lineages were, for the most part, well defined with mtDNA but not with nuDNA (Fig. 5). In the mtDNA SplitsTree network, all individual lineages were well supported (bs = 95–100) with the exception of lineage J, which was moderately supported (bs = 69; Fig. 5). A split that grouped one individual of lineage L with lineage K also was recovered as highly supported (bs = 89; Fig. 5). Additionally, Clades I and II were both recovered as highly supported (Clade I bs = 70, Clade II bs = 91), whereas Clade III was only moderately supported (bs = 67, Fig. 5). However, a subclade within Clade III comprising lineages I, J, K, and L, to the exclusion of lineages G and H, was recovered as highly supported (bs = 100), and the subclade comprising lineages G and H was also recovered as highly supported (bs = 91; Fig. 5). The nuDNA SplitsTree networks were less resolved than mtDNA. Both the R35

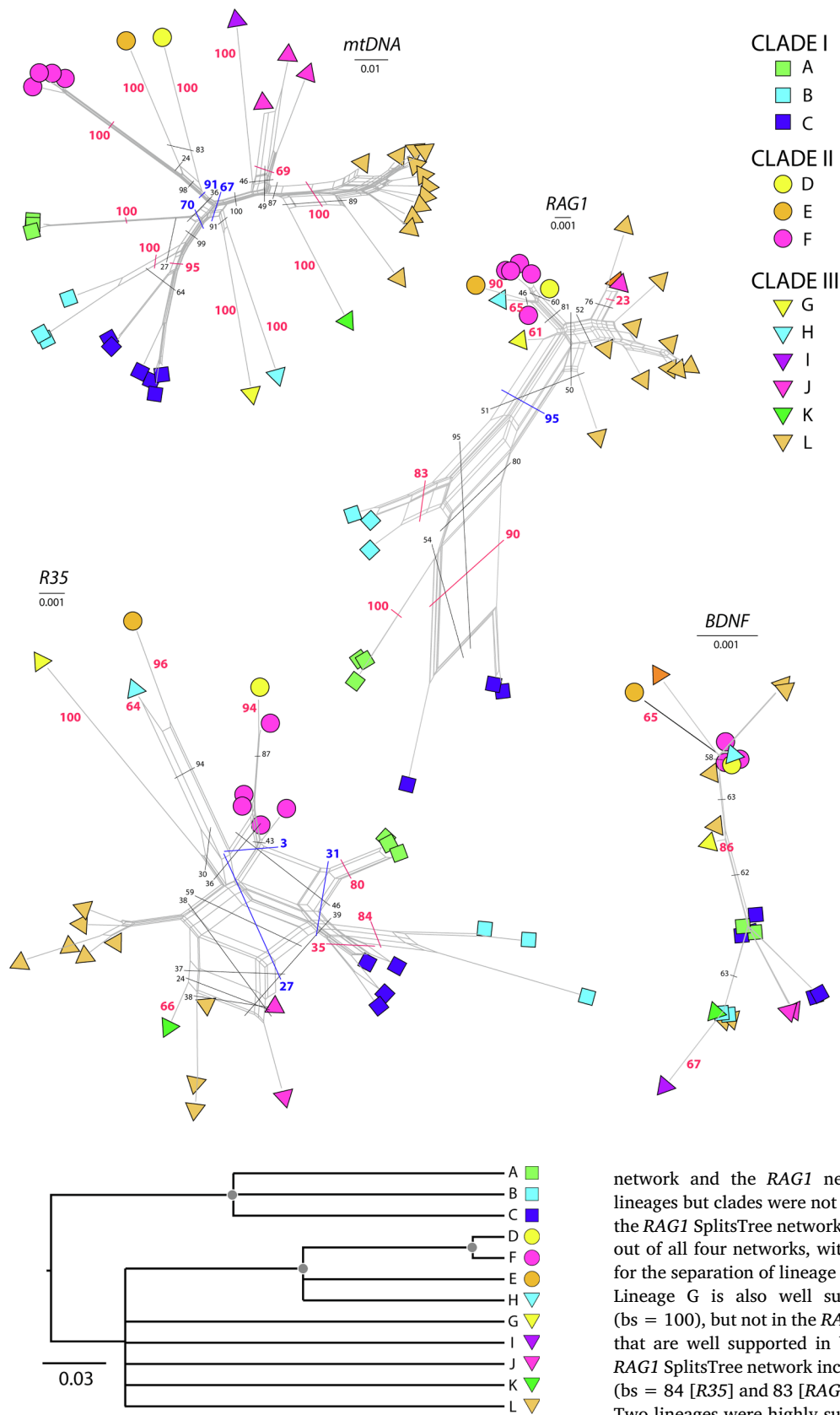


Fig. 6. Maximum clade credibility topology showing the results of the species tree analysis. Gray circles indicate nodes that are highly supported ($p \geq 0.95$). The scale bar indicates branch lengths in coalescent units.

Fig. 5. SplitsTree network graphs illustrating genetic splits for four loci: mitochondrial DNA (*mtDNA*) and the nuclear genes *BDNF*, *RAG1*, and *R35*. Gray lines represent the topology of each network, and blue, pink, and black lines crossing over the gray lines indicate major splits between taxa on either side of the line, with blue representing splits between clades, pink representing splits between lineages, and black representing other major splits. The color-coded number next to each colored line show the bootstrap support value for the split. Bootstrap support was assessed via 1000 bootstrap replicates and splits with values ≥ 70 are considered to be highly supported. (For interpretation of the references to color in this figure legend, the reader is referred to the web version of this article.)

network and the *RAG1* network had some support for individual lineages but clades were not supported, with the exception of Clade I in the *RAG1* SplitsTree network (bs = 95; Fig. 5). *BDNF* was least resolved out of all four networks, with the only instance of high support found for the separation of lineage G from all other lineages (bs = 86; Fig. 5). Lineage G is also well supported in the *R35* SplitsTree network (bs = 100), but not in the *RAG1* SplitsTree network (bs = 61). Lineages that are well supported in both the *R35* SplitsTree network and the *RAG1* SplitsTree network include A (bs = 80 [*R35*] and 100 [*RAG1*]), B (bs = 84 [*R35*] and 83 [*RAG1*]), and E (bs = 96 [*R35*] and 90 [*RAG1*]). Two lineages were highly supported only in a single nuDNA SplitsTree network: C (bs = 90 [*RAG1*]) and D (bs = 94 [*R35*]). Lineages that were not highly supported across any nuDNA SplitsTree network were lineages F, H, I, J, K, and L. Several of these lineages were represented by a single sample and did not amplify for every nuDNA gene (Table S3).

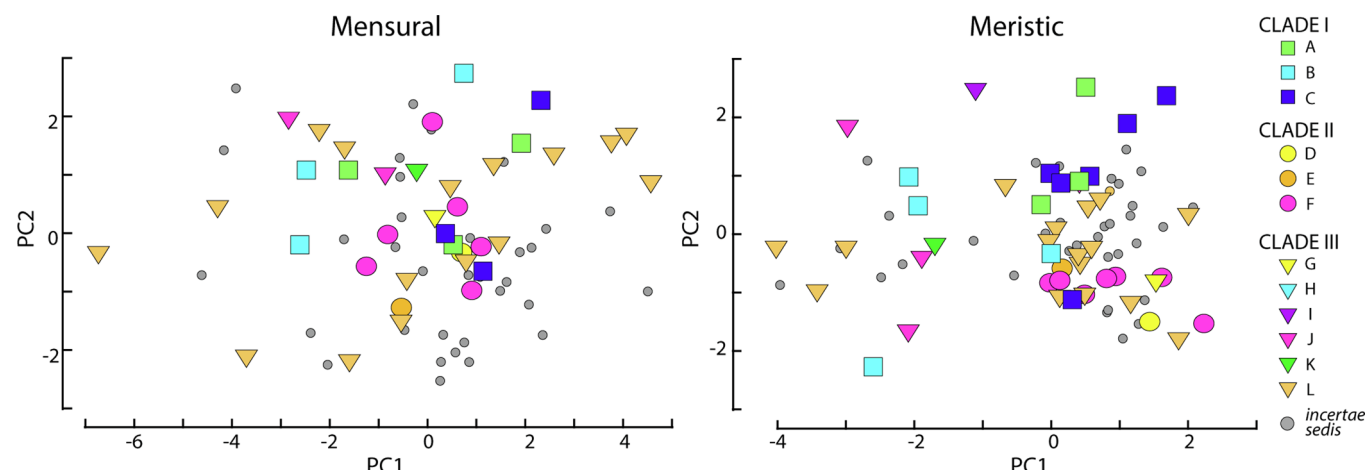


Fig. 7. Graphs of the mensural (left) and meristic (right) PCAs. Lineage H is not shown in the figure because the specimen was damaged and excluded from analyses.

3.4. Species tree

Species tree analysis of the 12 putative species obtained from BPP resulted in a topology with poorly supported structure (Fig. 6). Clade I is recovered with high support, although the relationships of lineage A, B, and C within Clade I are not resolved (Fig. 6). Clade II is also recovered with high support; however, lineage H is supported as part of Clade II, although its placement within the clade is not resolved (Fig. 6). Additionally, within Clade II, we recover lineages D and F as sister lineages (Fig. 6), which differs from the concatenated bModelTest analysis in which E and F are recovered as sister lineages, although this result in the concatenated analysis is only moderately supported ($pp = 0.93$; Fig. 3). A monophyletic Clade III is not recovered, with lineages G, I, J, K and L instead forming a polytomy along the backbone of the tree (Fig. 6).

3.5. Multivariate analyses of morphology

Results of the principal components analysis indicate that lineages and clades are not separated in morphospace (Fig. 7). In the mensural PCA analysis (Fig. 7), the first principal component (PC1) accounted for 36.5% of the variation and was loaded most heavily by TD, HW, HD, and FLL, suggesting that individuals are separated by body robustness, and the second principal component (PC2) accounted for 13.6% percent of the variation and loaded most heavily on AGD, MBW, TW, TD, END, and SNL, with AGD, MBW, TW, and TD negatively correlated with END and SNL, suggesting that individuals snout lengths are negatively correlated with body size (Table S6). Similarly, in the meristic PCA analysis (Fig. 7), PC1 accounted for 45.0% of the variation and loaded most heavily on MBSRC, PVSRC, FinIIIILam, and ToeIVLam, with FINIIILam and ToeIVLam negatively correlated with MBSRC and PVSRC, suggesting that body size is negatively correlated with digit length, and PC2 accounted for 21.1% percent of the variation and loaded most heavily on MBSRC and AGSRC, with MBSRC negatively correlated with AGSRC, suggesting that as the body elongates, body robustness decreases, and indicating that the degree of body elongation is important in distinguishing individuals in morphospace (Table S6). In the results of the meristic PCA, there does appear to be some separation of individuals along PC1 (Fig. 7); however, this separation does not correspond to phylogenetic placement and may be an artifact of the low samples size for some lineages. Clades or lineages do not form distinct clusters in morphospace in either the mensural or the meristic analysis. Lineage H, represented by a single sample, was excluded from both mensural and meristic analyses because the specimen was damaged. Lineage I was excluded from the mensural analysis because of its small size and damage, but it was included in the meristic analysis.

4. Discussion

4.1. Genetic and morphological diversity within *Myanmar Riopa*

Overall, we find high levels of genetic diversity within *Myanmar Riopa* that are not consistent with previously recognized morphological species boundaries. Currently, four species in the genus are recognized to occur in the country based on morphology: *R. albopunctata*, *R. anguina*, *R. lineolata*, and *R. popae*. However, results from our species delimitation analyses suggest that Myanmar harbors as many as 13 unique evolutionary lineages—the morphologically distinct *R. albopunctata*, plus 12 putative lineages recovered in species delimitation analyses that comprise the *R. anguina-lineolata-popae* species complex. Our concatenated and coalescent phylogenetic results indicate that these 12 lineages form a clade, sister to *R. albopunctata* (Fig. 3), which suggests that *Myanmar Riopa* has diversified *in situ* within the country. These 12 lineages of the *R. anguina-lineolata-popae* species complex are separated by *ND2* mitochondrial distances of 7.2–15.7% (Table 2) and are well supported by the mtDNA SplitsTree network analysis (Fig. 5). However, their support among nuDNA SplitsTree network analyses varies, with several lineages (A, B, E, G) supported by two out of three nuDNA SplitsTree networks, two lineages (C, D) supported by one nuDNA SplitsTree network, and the remaining six lineages (F, H, I, J, K, L) not supported by any of the nuDNA SplitsTree networks (Fig. 5). These results are not surprising given that mtDNA evolves at a faster rate than nuDNA (Wawter and Brown, 1986). The species delimitation program BPP is known to delimit population-level structure in addition to species-level structure (Sukumaran and Knowles, 2017; Barley et al., 2018; Luo et al., 2018; Leaché et al., 2019), and therefore, the lack of resolution among our nuDNA networks may indicate that some of the recovered lineages are genetically structured populations or incipient species instead of full species. Additionally, the species tree analysis does not fully resolve inter-lineage relationships (Fig. 5), which may be an artifact of low genetic sampling, or again, indicate that the lineages are incipient species.

Riopa species are small, cryptically colored, and semi-fossorial (Das, 2010), making them hard to detect during field surveys. As a result, one-half of the lineages recovered in species delimitation analyses (D, G, E, H, I, K) are represented in the dataset by a single individual, which prevents us from being able to characterize intra-lineage genetic diversity at this time. Furthermore, geographic sampling gaps exist across much of Myanmar, including in low–mid elevation regions in the eastern and southern portions of the country, and it is likely that additional unsampled genetic lineages exist within these regions. Species delimitation methods are affected by the taxonomic and geographic scope of sampling, and many do not accommodate low intra-specific

sampling (Lim et al., 2012), which affects their accuracy. As a result, the small sample size of many of our lineages (average $n = 3.4 \pm 3.8$) combined with the possibility of unsampled lineages in Myanmar may distort the signal of population- versus species-level diversity. Understanding the distributions of Myanmar *Riopa* is crucial to appreciating the evolutionary history of the group, therefore additional surveys targeting *Riopa* across the country are needed to better resolve population- and species-level diversity within this clade.

Despite the high amount of genetic diversity within Myanmar *Riopa*, we do not find that lineages or clades are separated in morphospace (Fig. 6). Instead, both the mensural and meristic PCAs show that there are no consistent morphological trends across lineages or clades. In the PC1 loadings for the mensural PCA and PC2 loadings for the meristic PCA, we do find the expected trend that body robustness is negatively correlated with body elongation across individuals (Gans, 1975; Wiens and Slingluff, 2001), but the other PC loadings are more difficult to interpret (Table S6). Additionally, no lineages are separated by qualitative head scalation patterns, with the exception of lineage F, in which all examined members have a scaly lower eyelid instead of a lower eyelid with a transparent disc. However, the taxonomic value of the lower eyelid state is a matter of debate due to its variability within clades (e.g. Broadley, 1966; Linkem et al., 2011; Freitas et al., 2019), with the state reportedly varying even between eyelids on the same individual (Hora, 1927). These morphological results suggest that intra-lineage morphology varies at least as much as inter-lineage morphology and indicates that body morphology is conservative across *Riopa* lineages in Myanmar, highlighting the limitations to employing diagnostic characters traditionally used in species delimitations studies in skinks.

Our qualitative head scalation patterns are coded in a binary fashion (e.g. presence versus absence); however, geometric morphometric analyses on skull characteristics have been shown to be a useful tool in separating species that appear qualitatively similar (Ruane, 2015; Rej and Mead, 2017; Gabelaia et al., 2018) and may help to differentiate lineages of Myanmar *Riopa* in future studies. Furthermore, we did not examine internal osteological characters or hemipenes morphology, character sets that have helped to distinguish species in other squamate systematic studies (Welton et al., 2010; Prötzl et al., 2018), and researchers undertaking future studies on *Riopa* may wish to include these additional morphological elements.

4.2. Biogeographic patterns within Myanmar *Riopa*

Myanmar is both geographically and geologically complex, comprising multiple regions of tectonic uplift resulting from the collision of the Indian subcontinent with the Laurasian subcontinent beginning approximately 52 million years ago (van Hinsbergen et al., 2012; Khin et al., 2017), with some eastern topographical features such as the Shan Plateau (Fig. 1) dating to the Late Cretaceous (reviewed in Licht, 2013). This complex landscape has contributed to high levels of endemism in other groups of squamate reptiles, including two genera of geckos in Myanmar: *Cyrtodactylus* (e.g. Grismer et al., 2018a) and *Hemiphyllodactylus* (e.g. Grismer et al., 2018b), and may have driven diversification of Myanmar *Riopa* in the western and central parts of the country. Based on the localities of sampled specimens (Fig. 1), it appears that most putative Myanmar *Riopa* species are allopatric, with the possible exceptions of lineages J and L on the western side of the Irrawaddy (Ayeyarwady) River and lineages B, G, and I at Mount Popa (Fig. 1). Despite their close proximity, lineages J and L are separated by *ND2* genetic distances of 7.2–9.3%, and lineages B, G, and I separated by *ND2* genetic distances of 11.1–14.0% and may represent instances of secondary contact between lineages that diverged in allopatry.

Lineages A and C are separated from the rest of Myanmar *Riopa* by the Arakan Yoma and Chin Hills, mountains that, along with the Naga Hills to the north, form the Indo-Myanmar (Indo-Burma) Range (Fig. 1). Uplift of the Indo-Myanmar Range began approximately 37 million

years ago, resulting from the collision of the Indian subcontinent with the Laurasian subcontinent (Mitchell, 1993; Licht et al., 2013). These mountains separate the western coast of Myanmar (the Assam Basin) from the country's interior Central Myanmar (Central Burma) Basin. Although the timing of the complete separation of the Central Myanmar Basin from the Assam Basin remains unknown (Licht et al., 2013), it is likely that biotic exchange could have occurred between the two regions until as recently as the early Oligocene, approximately 33 million years ago (Licht et al., 2013). This separation most likely predates the divergence of lineages A and C from the rest of Myanmar *Riopa*, suggesting that there was an instance of trans-mountain dispersal early in the diversification of the clade. The mountains in the southern Indo-Myanmar Range reach an elevation of over 3,000 m at Nat Ma Taung (Mount Victoria). Elevation data taken in the field for a subset of *Riopa* specimens indicates that individuals were found predominately at mid-elevations, with some individuals found at higher elevations (77–2,065 m above sea level; Table S3), suggesting that parts, but not all, of the Arakan Yoma and Chin Hills may be a barrier to dispersal between eastern and western lineages. Additionally, orographic lift of monsoon winds on the western side of the mountains results in the rain shadow effect in which the Assam Basin in the west is wetter than the Central Myanmar Basin in the east (Fig. 2), potentially exposing lineages A and C to a different set of ecological conditions than what is experienced by other members of Myanmar *Riopa*, although detailed ecological data on this group are not available.

Lineage B in Clade I and all lineages within Clades II and III are located in the central and southern portions of the Central Myanmar Basin, east of the Indo-Myanmar Range (Fig. 1). Within the southern and central portion of the Central Myanmar Basin, lineages B, E, G, H, J, and L are separated from each other by the Irrawaddy River, with B, E, G, and H found on the eastern side of the river and J and L found on the western side of the river. Lineages D, F, and K are located in the northern Central Myanmar Basin between the Chindwin and Irrawaddy Rivers. Although rivers have been implicated as barriers to dispersal of skinks in other parts of the world (Jackson and Austin, 2010; Miralles and Carranza, 2010; but see Vences et al., 2014), this is the first study recognizing the Irrawaddy River as a potential barrier to dispersal. Future studies focusing on gene flow between lineages on eastern and western sides of the river are needed to elucidate the role of the Irrawaddy River as a biogeographic barrier in Myanmar *Riopa*.

In addition to geographical boundaries, Myanmar has experienced changes in climate throughout the Miocene, Pliocene and Pleistocene, resulting from the uplift of the Himalayas and the subsequent strengthening of the South and East Asian monsoon systems (Clift et al., 2008; Zhang et al., 2015). Simulation studies suggest that the Chin Hills and the Arakan Yoma affect the climates of the Assam and Central Myanmar Basins by playing a critical role in the strengthening and seasonality of the annual South Asian Monsoon across the Indian subcontinent (Wu et al., 2014; Wu and Hsu, 2016). These climate changes caused a transition from C3- to C4-dominated grasslands (Quade et al., 1989) and gave rise to mosaic savannah forest habitat across the Indian Subcontinent and Southeast Asia (Sun and Wang, 2005; Patnaik and Nanda, 2010; Louys and Meijaard, 2010; Ratnam et al., 2016). Fossil ungulates and hominids from Pliocene and Pleistocene deposits in South and Southeast Asia provide additional evidence for the expansion of grassland habitats in the region during this time (Takai et al., 2006; Suraprasit et al., 2014; Patnaik, 2016). Species of *Riopa* are typically found in dry to semi-dry forests and grasslands (Das, 2010; Vyas, 2014; Bhattarai et al., 2018; Prasad et al., 2018), and populations may have been isolated by patches of forest habitats as vegetation shifts occurred throughout the Tertiary, thus promoting speciation under a scenario of reduced or suspended gene flow.

Across portions of the Central Myanmar Basin, precipitation falls below 1000 mm per year (Fig. 2C; Matsuda, 2013), forming a region of semi-arid habitat known as the Central Dry Zone (Figs. 1 and 2; Wu et al., 2014). This region has unique arid-adapted forest and grassland

habitats and high levels of endemism within terrestrial vertebrates (Grismer et al., 2018a; Platt et al., 2003; Poyarkov et al., 2019; Shimada et al., 2010; Slowinski and Wüster, 2000; Smith, 1943; Zug et al., 2006) and has been hypothesized as a major center of speciation (Zug et al., 2006); however, the mechanisms behind the high levels of diversification in this region remain unknown. Our results supporting multiple cryptic lineages of *Riopa* concentrated within the boundaries of the Central Dry Zone (lineages B, G, H, I, J, L; Figs. 1 and 2C) provide further evidence for the important role this biogeographic region may have played in vertebrate diversification.

4.3. Are Myanmar *Riopa* an example of non-ecological diversification?

The pattern of high genetic diversity with no accompanying morphological differentiation suggests that Myanmar *Riopa* have undergone non-ecological diversification, in which genetic divergence between lineages has not been driven by adaptation to divergent environmental conditions. Non-ecological diversification results from allopatric separation of populations into isolated ecologically similar regions, followed by non-ecologically mediated genetic evolution over time (Pyron et al., 2015; Czekanski-Moir and Rundell, 2019). Given the lack of morphological separation between lineages of Myanmar *Riopa*, it does not appear that lineages have been subjected to divergent natural selection or have undergone disparification (increase in morphospace area occupied over time by a clade [Czekanski-Moir and Rundell, 2019]) despite genetic diversification (Table 2). However, the lack of ecological data for Myanmar *Riopa* preclude the possibility of statistical tests of ecological differentiation within the clade, and we also lack knowledge on which morphological characters are ecologically relevant in the genus. It is possible that ecologically relevant variation exists between individuals but was not examined in this study. Additionally, we lack fossil data that could provide concrete evidence of ancestral morphology, an important consideration of whether diversification has been driven by ecological or non-ecological processes, although given the morphological uniformity of lineages within the clade, we hypothesize that the current morphology is plesiomorphic.

Signatures of non-ecological speciation have been documented in other groups of skinks including *Eutropis* in the Philippines (Barley et al., 2013), *Carlia* and *Lampropholis* in Australia (Singhal et al., 2018), and *Cryptoblepharus* in Australia (Blom et al., 2016). Similar to our observations, these studies reveal high levels of genetic diversification not accompanied by morphological disparification, although only Blom et al. (2016) conducted explicit statistical tests linking the morphology examined in the study with species' ecologies. In addition to these studies, the numerous instances of cryptic radiations across the Family Scincidae (see Table S1 for a list of all cryptic species described between 2014–2019) allude to non-ecological speciation as a common occurrence within scincid lizards, but this has not been tested explicitly in a statistical framework. Therefore, although it is clear that Myanmar *Riopa* constitutes a cryptic radiation, the processes contributing to diversification in the clade cannot be determined based on our current data.

4.4. Taxonomic implications

In discussing distribution patterns of *Riopa* species in Myanmar, Jayaram (1949:407) remarked, "it is likely that these are mere races of a single species." Our genetic results dispute this hypothesis and instead suggest that there is significant cryptic diversity present within the *R. anguina-lineolata-popae* species complex. However, because the species delimitation program BPP delimits both population- and species-level structure (Sukumaran and Knowles, 2017; Barley et al., 2018; Luo et al., 2018; Leaché et al., 2019), it is likely that some of the 12 lineages represent genetically divergent populations and not full species. Furthermore, using genetic data alone to diagnose species remains controversial (Bauer et al., 2011; Singhal et al., 2018; Hillis, 2019) despite

the widespread adoption of the General Lineage Concept definition of species (de Queiroz, 1998, 1999), which states only that species are independently evolving lineages.

Therefore, determination of which of our Myanmar *Riopa* lineages represent new species is complicated by the lack of distinguishing morphological features and the current paucity of other pertinent natural history information, such as behavior, ecology, microhabitat preferences, and geographic distributions. The type specimens of *R. anguina*, *R. lineolata*, and *R. popae* are housed at the Zoological Survey of India, the British Museum of Natural History, and the Museum of Comparative Zoology, respectively, and, except for *R. popae*, were not available for examination. Additionally, three sampled lineages were found at Mount Popa, the type locality of *R. popae* (lineages B, G, and I) and one sampled lineage (lineage B) was found around the approximate type locality of *R. anguina*, but no genetic samples exist from the type locality of *R. lineolata* (Fig. 1), making it difficult to assign lineages to recognized species based on their geographical distributions.

Additional studies are needed to determine what proportion of lineages identified within the *R. anguina-lineolata-popae* species warrant recognition as separate species. Because several lineages are found in close proximity with large genetic differentiation (J and L; B, G, and I; Fig. 1, Table 2), it is likely that they represent distinct species along separate evolutionary trajectories, according to the General Lineage Concept (de Queiroz, 1998, 1999). However, at this time, we decline to advance the taxonomy of this group until more data are available that will allow for improved resolution of species-level diversity within the *R. anguina-lineolata-popae* species complex. Recognizing the high levels of cryptic diversity with Myanmar *Riopa* is a critical first step in understanding the evolutionary dynamics that generate biodiversity in the region.

CRediT authorship contribution statement

Elyse S. Freitas: Conceptualization, Methodology, Investigation, Formal analysis, Writing - original draft, Writing - review & editing, Funding acquisition. **Aryeh H. Miller:** Conceptualization, Investigation, Writing - review & editing, Funding acquisition. **R. Graham Reynolds:** Writing - review & editing, Supervision, Funding acquisition. **Cameron D. Siler:** Conceptualization, Writing - review & editing, Supervision, Funding acquisition.

Acknowledgements

This research was made possible by a joint collaboration between the California Academy of Sciences (CAS), the National Museum of Natural History (NMNH) and the Smithsonian Institution, and the Ministry of Forestry, Department of Forestry, Myanmar Nature and Conservation Division (NWCD) who formed a Myanmar herpetology survey team of rangers under the supervision of J. Vindum. For tissue and specimen loans (Table S3), we thank J. Vindum and L. Scheinberg at CAS, L. Grismer at the La Sierra University Herpetology Collection (LSUHC), C. Spencer at the Museum of Vertebrate Zoology (MVZ), A. Datta-Roy at the National Institute of Science Education and Research (NISER), and A. Bauer at Villanova University. We thank L. Scheinberg at CAS, A. Resetar at the Field Museum of Natural History (FMNH), and J. Rosado at the Museum of Comparative Zoology (MCZ) for facilitating collection visits for AHM. We are grateful to T. Yuri, M. Labonte and M. Penrod at the Sam Noble Oklahoma Museum of Natural History (SNOMNH) for help with molecular data collection. We thank J. Oaks for discussion of methods and help with *BEAST2 and bModelTest analyses and appreciate additional help provided by the Taming the BEAST 2018 workshop in Oberägeri, Switzerland. We also appreciate J. Lee, D. Mulcahy and G. Zug for helpful discussions on skinks in Myanmar. Fieldwork in Myanmar was funded by NSF grant DEB 9971861 to J. Slowinski and G. Zug and DEB 0451832 to A. Leviton, J. Vindum, and G. Zug. This research was supported by the University of

Oklahoma Alumni Funds, Graduate Student Senate Award, and Department of Herpetology Loren G. Hill Fund to ESF; funds from the University of North Carolina Asheville to AHM and RGR; and NSF grants IOS 1353683 and DEB 1657648 to CDS. Finally, we are very grateful to the two anonymous reviewers who gave us feedback, which greatly improved our manuscript.

Appendix A. Supplementary material

Supplementary data to this article can be found online at <https://doi.org/10.1016/j.ympev.2020.106754>.

References

Aljanabi, S.M., Martinez, I., 1997. Universal and rapid salt-extraction of high quality genomic DNA for PCR-based techniques. *Nucleic Acids Res.* 25, 4692–4693. <https://doi.org/10.1093/nar/25.22.4692>.

Barley, A.J., White, J., Diesmos, A.C., Brown, R.M., 2013. The challenge of species delimitation at the extremes: diversification without morphological change in Philippine sun skinks. *Evolution* 67, 3556–3572. <https://doi.org/10.1111/evol.12219>.

Barley, A.J., Brown, J.M., Thomson, R.C., 2018. Impact of model violations on the inference of species boundaries under the multispecies coalescent. *Syst. Biol.* 67, 269–284. <https://doi.org/10.1093/sysbio/syx073>.

Bauer, A.M., Parham, J.F., Brown, R.M., Stuart, B.L., Grismer, L.L., Papenfuss, T.J., Böhme, W., Savage, J.M., Carranza, S., Grismer, J.L., Wagner, P., Schmitz, A., Ananjeva, N.B., Inger, R.F., 2011. Availability of new Bayesian-delimited gecko names and the importance of character-based species descriptions. *Proc. R. Soc. B* 278, 490–492. <https://doi.org/10.1098/rspb.2010.1330>.

Bhattarai, S., Pokhrel, C.P., Lamichhane, B.R., Regmi, U.R., Ram, A.K., Subedi, N., 2018. Amphibians and reptiles of Parsa National Park, Nepal. *Amphib. Reptile Conserv.* 12, 35–48.

Bickford, D., Lohman, D.J., Sodhi, N.S., Ng, P.K.L., Meier, R., Winker, K., Ingram, K.K., Das, I., 2007. Cryptic species as a window on diversity and conservation. *Trends Ecol. Evol.* 22, 148–155. <https://doi.org/10.1016/j.tree.2006.11.004>.

Blom, M.P.K., Horner, P., Moritz, C., 2016. Convergence across a continent: adaptive diversification in a recent radiation of Australian lizards. *Proc. R. Soc. B* 283, 20160181. <https://doi.org/10.1098/rspb.2016.0181>.

Bortolus, A., 2008. Error cascades in the biological sciences: the unwanted consequences of using bad taxonomy in ecology. *Ambio* 37, 114–118. [https://doi.org/10.1579/0044-7447\(2008\)37\[114:ECITBS\]2.0.CO;2](https://doi.org/10.1579/0044-7447(2008)37[114:ECITBS]2.0.CO;2).

Bouckaert, R., Heled, J., Kühnert, D., Vaughan, T., Wu, C.H., Xie, D., Suchard, M.A., Rambaut, A., Drummond, A.J., 2014. BEAST 2: a software platform for Bayesian evolutionary analysis. e1003537. *PLOS Comput. Biol.* 10. <https://doi.org/10.1371/journal.pcbi.1003537>.

Bouckaert, R.R., Drummond, A.J., 2017. bModelTest: Bayesian phylogenetic site model averaging and model comparison. *BMC Evol. Biol.* 17, 42. <https://doi.org/10.1186/s12862-017-0890-6>.

Brandley, M.C., Ota, H., Hikida, T., de Oca, A.N.M., Feria-Ortiz, M., Guo, X., Wang, Y., 2012. The phylogenetic systematics of blue-tailed skinks (*Plestiodon*) and the family Scincidae. *Zool. J. Linn. Soc.* 165, 163–189. <https://doi.org/10.1111/j.1096-3642.2011.00801.x>.

Broadley, D.G., 1966. A review of the *Riopa sundevalli* group (Sauria: Scincidae) in southern Africa. *Arnoldia (Rhodesia) Series of Miscellaneous Publications National Museums of Southern Rhodesia* 2 (34), 1–7.

Brown, S.D.J., Collins, R.A., Boyer, S., Lefort, M.C., Malumbres-Olarte, J., Vink, C.J., Cruickshank, R.H., 2012. SPIDER: an R package for the analysis of species identity and evolution, with particular reference to DNA barcoding. *Mol. Ecol. Resour.* 12, 562–565. <https://doi.org/10.1111/j.1755-0998.2011.03108.x>.

Bryant, D., Moulton, V., 2004. Neighbor-Net: an agglomerative method for the construction of phylogenetic networks. *Mol. Biol. Evol.* 21, 255–265. <https://doi.org/10.1093/molbev/msh018>.

Cerfaco, L.M.P., Gutiérrez, E.E., Dubois, A., 2016. Photography-based taxonomy is inadequate, unnecessary, and potentially harmful for biological sciences. *Zootaxa* 4196, 435–445. <https://doi.org/10.11646/zootaxa.4196.3.9>.

Chan-ard, T., Parr, J.W.K., Nanhithabha, J., 2015. *A Field Guide to the Reptiles of Thailand*. Oxford University Press, New York.

Clift, P.D., Hodges, K.V., Heslop, D., Hannigan, R., van Long, H., Calves, G., 2008. Correlation of Himalayan exhumation rates and Asian monsoon intensity. *Nat. Geosci.* 1, 875–880. <https://doi.org/10.1038/ngeo351>.

Czekanski-Moir, J.E., Rundell, R.J., 2019. The ecology of nonecological speciation and nonadaptive radiations. *Trends Ecol. Evol.* 34, 400–415. <https://doi.org/10.1016/j.tree.2019.01.012>.

Das, I., 2010. *A Field Guide to the Reptiles of Southeast Asia*. New Holland, London.

Datta-Roy, A., Singh, M., Karanth, K.P., 2014. Phylogeny of endemic skinks of the genus *Lygosoma* (Squamata: Scincidae) from India suggests an in situ radiation. *J. Genet.* 93, 163–167.

de Queiroz, K., 1998. The general lineage concept of species, species criteria, and the process of speciation. A conceptual unification and terminological recommendations. In: Howard, D.J., Berlocher, S.H. (Eds.), *Endless Forms: Species and Speciation*. Oxford University Press, New York, pp. 57–75.

de Queiroz, K., 1999. The general lineage concept of species and the defining properties of the species category. In: Wilson, R.A. (Ed.), *Species: New Interdisciplinary Essays*. MIT Press, Cambridge, pp. 49–89.

de Queiroz, K., 2005. Ernst Mayr and the modern concept of species. *Proc. Natl. Acad. Sci.* 102, 6600–6607. <https://doi.org/10.1073/pnas.0502030102>.

Denham, S.S., Brignone, N.F., Johnson, L.A., Pozner, R.E., 2019. Using integrative taxonomy and multispecies coalescent models for phylogeny reconstruction and species delimitation with the “*Nastanthus-Gamocarpha*” clade (Calyceraceae). *Mol. Phylogenet. Evol.* 130, 211–226. <https://doi.org/10.1016/j.ympev.2018.10.015>.

Drummond, A.J., Suchard, M.Z., 2010. Bayesian random local clocks, or one rate to rule them all. *BMC Biol.* 8, 114. <https://doi.org/10.1186/1741-7007-8-114>.

Dubois, A., 2003. The relationships between taxonomy and conservation biology in the century of extinctions. *C. R. Biol.* 326, s9–s21. [https://doi.org/10.1016/S1631-0691\(03\)00022-2](https://doi.org/10.1016/S1631-0691(03)00022-2).

Duran, D.P., Herrmann, D.P., Roman, S.J., Gwiazdowski, R.A., Drummond, J.A., Hood, G.R., Egan, S.P., 2019. Cryptic diversity in the North American *Dromochorus* tiger beetles (Coleoptera: Carabidae: Cicindelinae): a congruence-based method for species discovery. *Zool. J. Linn. Soc.* 186, 250–285. <https://doi.org/10.1093/zoolinnean/zly035>.

Edgar, R.C., 2004. MUSCLE: multiple sequence alignment with high accuracy and high throughput. *Nucleic Acids Res.* 32, 1792–1797. <https://doi.org/10.1093/nar/gkh340>.

Erens, J., Miralles, A., Glaw, F., Chatrou, L.X., Vences, M., 2017. Extended molecular phylogenetics and revised systematics of Malagasy scincine lizards. *Mol. Phylogenet. Evol.* 107, 466–472. <https://doi.org/10.1016/j.ympev.2016.12.008>.

Flouri, T., Jiao, X., Rannala, B., Yang, Z., 2018. Species tree inference with BPP using genomic sequences and the multispecies coalescent. *Mol. Biol. Evol.* 35, 2585–2593. <https://doi.org/10.1093/molbev/msy147>.

Frankham, R., Ballou, J.D., Dudash, M.R., Eldridge, M.D.B., Fenster, C.B., Lacy, R.C., Mendelson III, J.R., Porton, I.J., Ralls, K., Ryder, O.A., 2012. Implications of different species concepts for conserving biodiversity. *Biol. Conserv.* 153, 25–31. <https://doi.org/10.1016/j.biocon.2012.04.034>.

Freitas, E.S., Datta-Roy, A., Karanth, P., Grismer, L.L., Siler, C.D., 2019. Multilocus phylogeny and a new classification for African, Asian, and Indian supple and writhing skinks (Scincidae: Lygosominae). *Zool. J. Linn. Soc.* 186, 1067–1096. <https://doi.org/10.1093/zoolinnean/zlz001>.

Fry, B.G., Vidal, N., Norman, J.A., Vonk, F.J., Scheib, H., Ramjan, S.F.R., Kuruppu, S., Fung, K., Hedges, S.B., Richardson, M.K., Hodgson, W.C., Ignjatovic, V., Summerhayes, R., Kochva, E., 2006. Early evolution of the venom system in lizards and snakes. *Nature* 439, 584–588. <https://doi.org/10.1038/nature04328>.

Gabelaia, M., Tarkhnishvili, D., Adriaens, D., 2018. Use of three-dimensional geometric morphometrics for the identification of closely related species of rock lizards (Lacertidae: *Darevskia*). *Biol. J. Linn. Soc.* 125, 709–717. <https://doi.org/10.1093/biolinnean/bly143>.

Gans, C., 1975. Tetrapod limblessness: evolution and functional corollaries. *Amer. Zool.* 15, 455–467. <https://doi.org/10.1093/icb/15.2.455>.

Garnett, S.T., Christidis, L., 2017. Taxonomy anarchy hampers conservation. *Nat.* 546, 25–27. <https://doi.org/10.1038/546025a>.

Geissler, P., Hartmann, T., Neang, T., 2012. A new species of the genus *Lygosoma* Hardwicke & Gray, 1827 (Squamata: Scincidae) from northeastern Cambodia, with an updated identification key to the genus *Lygosoma* in mainland Southeast Asia. *Zootaxa* 3190, 56–68. <https://doi.org/10.11646/zootaxa.3190.1>.

Grismer, L.L., Wood Jr., P.L., Thura, M.K., Zin, T., Quah, E.S.H., Murdoch, M.L., Grismer, M.S., Lin, A., Kyaw, H., Lwin, N., 2018b. Twelve new species of *Cyrtodactylus* Gray (Squamata: Gekkonidae) from isolated limestone habitats in east-central and southern Myanmar demonstrate high localized diversity and unprecedented micro-endemism. *Zool. J. Linn. Soc.* 182, 862–959. <https://doi.org/10.1093/zoolinnean/zlx057>.

Hillis, D.M., Bull, J.J., 1993. An empirical test of bootstrapping as a method for assessing confidence in phylogenetic analysis. *Syst. Biol.* 42, 182–192. <https://doi.org/10.1093/sysbio/42.2.182>.

Grismer, L.L., Wood Jr., P.L., Quah, E.S., Murdoch, M.L., Grismer, M.S., Herr, M.W., Espinoza, R.E., Brown, R.M., Lin, A., 2018a. A phylogenetic taxonomy of the *Cyrtodactylus peguensis* group (Reptilia: Squamata: Gekkonidae) with descriptions of two new species from Myanmar. e5575. *PeerJ* 6. <https://doi.org/10.7717/peerj.5575>.

Grismer, L.L., Wood Jr., P.L., Thura, M.K., Zin, T., Quah, E.S.H., Murdoch, M.L., Grismer, M.S., Li, A., Kyaw, H., Lwin, N., 2018c. Phylogenetic taxonomy of *Hemiphyllodactylus* Bleeker, 1860 (Squamata: Gekkonidae) with descriptions of three new species from Myanmar. *J. Nat. Hist.* 52, 881–915. <https://doi.org/10.1080/00222933.2017.1367045>.

Hillis, D.M., 2019. Species delimitation in herpetology. *J. Herpetol.* 53, 3–12. <https://doi.org/10.1670/18-123>.

Hora, S.L., 1927. Notes on lizards in the Indian museum. III. On the unnamed collection of lizards of the family Scincidae. *Rec. Indian Mus.* 29, 1–6.

Huelsenbeck, J.P., Rannala, B., 2004. Frequentist properties of Bayesian posterior probabilities of phylogenetic trees under simple and complex substitution models. *Syst. Biol.* 53, 904–913. <https://doi.org/10.1080/10635150490522629>.

Huson, D.H., Bryant, D., 2006. Application of phylogenetic networks in evolutionary studies. *Mol. Biol. Evol.* 23, 254–267. <https://doi.org/10.1093/molbev/msj030>.

IUCN-SSC Species Conservation Planning Sub-Committee, 2017. Guidelines for Species Conservation Planning. Version 1.0. IUCN, Gland. <https://doi.org/10.2305/IUCN.CH.2017.18.en>.

Jackson, N.D., Austin, C.C., 2010. The combined effects of rivers and refugia generate extreme cryptic fragmentation within the common ground skink (*Scincella lateralis*). *Evolution* 64, 409–428. <https://doi.org/10.1111/j.1558-5646.2009.00840.x>.

Jayaram, K.C., 1949. Distribution of lizards of peninsular India with Malayan affinities. *Proc. Nat. Inst. Sci. India*. 15, 403–408, pl XV.

Khin, K., Zaw, K., Aung, L.T., 2017. Geological and tectonic evolution of the Indo-Myanmar Ranges (IMR) in the Myanmar region. In: Barbar, A.J., Zaw, K., Crow, M.J. (Eds.), Myanmar: Geology, Resources, and Tectonics. *Geol. Soc. London Mem.*, pp. 65–79 <https://doi.org/10.1144/M48.4>.

Knowlton, N., Jackson, J.B.C., 1994. New taxonomy and niche partitioning on coral reefs: jack of all trades or master of some? *Trends Ecol. Evol.* 9, 7–9. [https://doi.org/10.1016/0169-5347\(94\)90224-0](https://doi.org/10.1016/0169-5347(94)90224-0).

Leaché, A.D., McGuire, J.A., 2006. Phylogenetic relationships of horned lizards (*Phrynosoma*) based on nuclear and mitochondrial data: evidence for a misleading mitochondrial gene tree. *Mol. Phylogenet. Evol.* 39, 628–644. <https://doi.org/10.1016/j.ympev.2005.12.016>.

Leaché, A.D., Zhu, T., Rannala, B., Yang, Z., 2019. The spectre of too many species. *Syst. Biol.* 68, 168–181. <https://doi.org/10.1093/sysbio/syy051>.

Licht, A., France-Lanord, C., Reisberg, L., Fontaine, C., Soe, A.N., Jaeger, J.J., 2013. A palaeo Tibet-Myanmar connection? Reconstructing the Late Eocene drainage system of central Myanmar using a multi-proxy approach. *J. Geol. Soc. London*. 170, 929–939. <https://doi.org/10.1144/jgs2012-126>.

Lim, G.S., Balke, M., Meier, R., 2012. Determining species boundaries in a world full of rarity: singletons, species delimitation methods. *Syst. Biol.* 61, 165–169. <https://doi.org/10.1093/sysbio/syr030>.

Linnaeus, C., 1758. *Systema naturæ per regna tria naturæ, secundum classes, ordines, genera, species, cum characteribus, differentiis, synonymis, locis*. Tomus I. Editio decima, reformata. L. Salvius, Stockholm.

Linkem, C.W., Diesmos, A.C., Brown, R.M., 2011. Molecular systematics of Philippine forest skinks (Squamata: Scincidae: *Sphenomorphus*): testing morphological hypotheses of interspecific relationships. *Zool. J. Linn. Soc.* 163, 1217–1243. <https://doi.org/10.1111/j.1096-3642.2011.00747.x>.

Leonart, J., Salat, J., Torres, G.J., 2000. Removing allometric effects of body size in morphological analysis. *J. Theor. Biol.* 205, 85–93. <https://doi.org/10.1006/jtbi.2000.2043>.

Louys, J., Meijaard, E., 2010. Palaeoecology of Southeast Asian megafauna-bearing sites from the Pleistocene and a review of environmental changes in the region. *J. Biogeog.* 37, 1432–1449. <https://doi.org/10.1111/j.1365-2699.2010.02297.x>.

Luo, A., Ling, C., Ho, S.Y.W., Zhu, C.D., 2018. Comparison of methods for molecular species delimitation across a range of speciation scenarios. *Syst. Biol.* 67, 830–846. <https://doi.org/10.1093/sysbio/syy011>.

Manthey, U., Grossman, W., 1997. Amphibien & Reptilien Südostasiens. Natur und Tier—Verlag, Münster.

Macey, J.R., Larson, A., Ananjeva, N.B., Fang, Z., Papenfuss, T.J., 1997. Two novel gene orders and the role of light-strand replication in rearrangement of the vertebrate mitochondrial genome. *Mol. Biol. Evol.* 14, 91–104.

Matsuda, M., 2013. Upland farming systems coping with uncertain rainfall in the Central Dry Zone of Myanmar: how stable is indigenous multiple cropping under semi-arid conditions? *Hum. Ecol.* 41, 927–936. <https://doi.org/10.1007/s10745-013-9604-x>.

Meyer, C.P., Paulay, G., 2005. DNA barcoding: error rates based on comprehensive sampling. *e422*. *Plos Biol.* 3. <https://doi.org/10.1371/journal.pbio.0030422>.

Miller, M.A., Pfeiffer, W., Schwartz, T., 2010. Creating the CIPRES science gateway for inference of large phylogenetic trees. In: *Gateway Computing Environments Workshop 2010*. New Orleans: IEEE. <https://doi.org/10.1109/GCE.2010.5676129>.

Miralles, A., Carranza, S., 2010. Systematics and biogeography of the Neotropical genus *Mabuya*, with species emphasis on the Amazonian skink *Mabuya nigropunctata* (Reptilia, Scincidae). *Mol. Phylogenet. Evol.* 54, 857–869. <https://doi.org/10.1016/j.ympev.2009.10.016>.

Mitchell, A.H.G., 1993. Cretaceous-Cenozoic tectonic events in the western Myanmar (Burma)-Assam region. *J. Geol. Soc. London* 150, 1089–1102. <https://doi.org/10.1144/gsjgs.150.6.1089>.

Mittermeier, R.A., Myers, N., Mittermeier, C.G. (Eds.), 1999. *Hotspots: Earth's Biologically Richest and Most Endangered Terrestrial Ecoregions*. CEMEX, Mexico City.

Myers, N., 1988. Threatened biotas: “hot spots” in tropical forests. *Environmentalist* 8, 187–208. <https://doi.org/10.1007/BF02240252>.

Myers, N., 1990. The biodiversity challenge: expanded hot-spots analysis. *Environmentalist* 10, 243–256. <https://doi.org/10.1007/BF02239720>.

Myers, N., Mittermeier, R.A., Mittermeier, C.G., da Fonseca, G.A.B., Kent, J., 2000. Biodiversity hotspots for conservation priorities. *Nat.* 853–858. <https://doi.org/10.1038/35002501>.

Nabhitabha, J., Chan-ard, T., Chuaynkern, Y., 2000. Checklist of Amphibians and Reptiles in Thailand. Office of Environmental Policy and Planning, Bangkok, pp. 80–92.

Ogilvie, H.A., Bouckaert, R.R., Drummond, A.J., 2017. StarBEAT2 brings faster species tree inference and accurate estimates of substitution rates. *Mol. Biol. Evol.* 34, 2101–2114. <https://doi.org/10.1093/molbev/msx126>.

Palumbi, S., 1991. The simple fool's guide to PCR. Department of Zoology and Kewalo Marine Laboratory, Honolulu.

Paradis, E., Schliep, K., 2018. ape 5.0: an environment for modern phylogenetics and evolutionary analyses in R. *Bioinformatics* 35, 526–528. <https://doi.org/10.1093/bioinformatics/bty633>.

Patnaik, R., Nanda, A.C., 2010. Early pleistocene mammalian faunas of India and evidence of connections with other parts of the world. In: Fleagle, J.G., Shea, J.J., Grine, F.E., Baden, A.L., Leakey, R.E. (Eds.), *Out of Africa I: The First Hominin Colonization of Eurasia. Vertebrate Paleobiology and Paleoanthropology Series*. Springer, Dordrecht, pp. 129–143 <https://doi.org/10.1007/978-90-481-9036-2>.

Patnaik, R., 2016. Neogene-Quaternary mammalian paleobiogeography of the Indian subcontinent: an appraisal. *C. R. Palevol.* 15, 889–902. <https://doi.org/10.1016/j.crte.2016.01.004>.

Platt, S.G., Ko, W.K., Khaing, L.L., Myo, K.M., Swe, T., Lwin, T., Rainwater, T.R., 2003. Population status and conservation of the critically endangered Burmese star tortoise *Geochelone platynota* in central Myanmar. *Oryx* 37, 464–471. <https://doi.org/10.1017/S0030605303000838>.

Pons, J., Barracough, T.G., Gomez-Zurita, J., Cardoso, A., Duran, D.P., Hazell, S., Kamoun, S., Sunlin, W.D., Vogler, A.P., 2006. Sequences-based species delimitation for the DNA taxonomy of undescribed insects. *Syst. Biol.* 55, 595–609. <https://doi.org/10.1080/10635150600852011>.

Poyarov, J.N., Gorin, V.A., Zaw, T., Kretova, V.D., Gogoleva, S.S., Pawangkhanant, P., Che, J., 2019. On the road to Mandalay: contribution to the *Microhyla* Tschudi, 1838 (Amphibia: Anura: Microhylidae) fauna of Myanmar with description of two new species. *Zool. Res.* 40, 244–276. <https://doi.org/10.24272/j.issn.2095-8137.2019.044>.

Prasad, W.K., Verma, A., Shahabuddin, G., 2018. An annotated checklist of the herpetofauna of the Rashtrapati Bhawan Estates, New Delhi, India. *J. Threatened Taxa*. 10, 11295–11302. <https://doi.org/10.11609/jott.3235.10.2.11295-11302>.

Prötz, D., Heß, M., Scherz, M.D., Schwager, M., van't Padje, A., Glaw, F., 2018. Widespread bone-based fluorescence in chameleons. *Sci. Rep.* 8, 698. <https://doi.org/10.1038/s41598-017-19070-7>.

Pyron, R.A., Costa, G.C., Patten, M.A., Burbrink, F.T., 2015. Phylogenetic niche conservatism and the evolutionary basis of ecological speciation. *Biol. Rev.* 90, 1248–1262. <https://doi.org/10.1111/brv.12154>.

Quade, J., Cerling, T.E., Bowman, J.R., 1989. Development of Asian monsoon revealed by marked ecological shift during the latest Miocene in northern Pakistan. *Nat.* 342, 163–166. <https://doi.org/10.1038/342163a0>.

R Core Team, 2018. R: a language and environment for statistical computing. R Foundation for Statistical Computing. <https://www.R-project.org/>.

Rambaut, A., Drummond, A.J., Xie, D., Baele, G., Suchard, M.A., 2018. Posterior summarization in Bayesian phylogenetics using Tracer 1.7. *Syst. Biol.* 67, 901–904. <https://doi.org/10.1093/sysbio/syy032>.

Rannala, B., Yang, Z., 2003. Bayes estimation of species divergence times and ancestral population sizes using DNA sequences from multiple loci. *Genetics* 164, 1645–1656.

Ratnam, J., Tomlinson, K.W., Rasquinha, D.N., Sankaran, M., 2016. Savannahs of Asia: antiquity, biogeography, and an uncertain future. *Phil. Trans. R. Soc. B*. 371, 20150305. <https://doi.org/10.1098/rstb.2015.0305>.

Reid, N.M., Carstens, B.C., 2012. Phylogenetic estimation error can decrease the accuracy of species delimitation: a Bayesian implementation of the general mixed Yule-coalescent model. *BMC Evol. Biol.* 12, 196. <https://doi.org/10.1186/1471-2148-12-196>.

Reid, N.M., 2014. bGMYC: A Bayesian MCMC implementation of the general mixed Yule-coalescent model for species delimitation. R package version 1.0.2.

Rej, J.E., Mead, J.I., 2017. Geometric morphometric differentiation of two western USA lizards (Phrynosomatidae: Squamata): *Uta stansburiana* and *Urosaurus ornatus*, with implications for fossil identification. *Bull. Southern California Acad. Sci.* 116, 153–161. <https://doi.org/10.3160/soca-116-03-153-161.1>.

Ruane, S., 2015. Using geometric morphometrics for integrative taxonomy: an examination of head shapes of milksnakes (genus *Lampropeltis*). *Zool. J. Linn. Soc.* 174, 394–413. <https://doi.org/10.1111/zoj.12245>.

Seetharamaraju, M., Sreeker, R., Srinivasulu, C., Srinivasulu, B., Kaur, H., Venkateshwarlu, P., 2009. Rediscovery of Vosemer's Writhing Skink *Lygosoma vossmeri* (Gray, 1839) (Reptilia: Scincidae) with a note on its taxonomy. *J. Threatened Taxa*. 12, 624–626. <https://doi.org/10.11609/JoTT.02160.624-6>.

Seifan, M., Zohar, Y., Werner, Y.L., 2016. Reptile distribution may identify terrestrial islands for conservation: the Levant's Arava Valley as a model. *J. Nat. Hist.* 50, 2783–2801. <https://doi.org/10.1080/00222933.2016.1205154>.

Shimada, T., Aplin, K.P., Suzuki, H., 2010. *Mus lepidoides* (Muridae, Odontia) of Central Burma is a distinct species of potentially great evolutionary and biogeographic significance. *Zool. Sci.* 27, 449–459. <https://doi.org/10.2108/zsj.27.449>.

Shreve, B., 1940. Reptiles and amphibians from Burma with descriptions of three new skinks [sic]. *Proc. New Engl. Zool. Club.* 18, 17–26.

Siler, C.D., Diesmos, A.C., Alcalá, A.C., Brown, R.M., 2011. Phylogeny of Philippine slender skinks (Scincidae: *Brachymeles*) reveals underestimated species diversity, complex biogeographical relationships, and cryptic patterns of lineage diversification. *Mol. Phylogenet. Evol.* 59, 54–65. <https://doi.org/10.1016/j.ympev.2010.12.019>.

Siler, C.D., Diesmos, A.C., Brown, R.M., 2010. New loam-swimming skink, genus *Brachymeles* (Reptilia: Squamata: Scincidae) from Luzon and Catanduanes Islands, Philippines. *J. Herpetol.* 44, 49–60. <https://doi.org/10.1670/08-318.1>.

Singhal, S., Hoskin, C.J., Couper, P., Potter, S., Moritz, C., 2018. A framework for resolving cryptic species: a case study from the lizards of the Australian wet tropics. *Syst. Biol.* 67, 1061–1075. <https://doi.org/10.1093/sysbio/syy026>.

Skinner, A., Hutchinson, M.N., Lee, M.S.Y., 2013. Phylogeny and divergence times of Australian *Sphenomorphus* group skinks (Scincidae, Squamata). *Mol. Phylogenet. Evol.* 69, 906–918. <https://doi.org/10.1016/j.ympev.2013.06.014>.

Slowinski, J.B., Wüster, W., 2000. A new cobra (Elapidae: *Naja*) from Myanmar (Burma). *Herpetologica* 56, 257–270.

Smith, M.A., 1943. *The Fauna of British India, Ceylon and Burma, Including the Whole of the Indo-Chinese Sub-region. Reptilia and Amphibia, Vol. III-Serpentes*. Taylor and Francis, London.

Srinivasulu, C., Seetharamaraju, M., 2010. Reply to ‘further comments on the systematic status of *Lygosoma vossmeri* (Gray 1839)’ by Raju Vyas. *J. Threatened Taxa*. 2, 675. <https://doi.org/10.11609/JoTT.02390.675>.

Stamatakis, A., 2014. RAXML vol 8: a tool for phylogenetic analysis and post-analysis of large phylogenies. *Bioinform.* 30, 1312–1313. <https://doi.org/10.1093/bioinformatics/btu033>.

Stoliczka, F., 1870. *Observations on some Indian and Malayan Amphibia and Reptilia*. J.

Asiatic Soc. Bengal. 39 (134–228), x–xii.

Sukumaran, J., Knowles, L.L., 2017. Multispecies coalescent delimits structure, not species. Proc. Natl. Acad. Sci. 114, 1607–1612. <https://doi.org/10.1073/pnas.1607921114>.

Sun, X., Wang, P., 2005. How old is the Asian monsoon system? Palaeobotanical records from China. Palaeogeog. Palaeoclim. Palaeoecol. 222, 181–222. <https://doi.org/10.1016/j.palaeo.2005.03.005>.

Suraprasit, K., Chaimanee, Y., Bocherens, H., Chavasseau, O., Jaeger, J.J., 2014. Systematics and phylogeny of middle Miocene Cervidae (Mammalia) from Mae Moh Basin (Thailand) and a paleoenvironmental estimate using enamel isotopy of sympatric herbivore species. J. Vertebr. Paleontol. 34, 179–194. <https://doi.org/10.1080/02724634.2013.789038>.

Takai, M., Saeusa, H., Htike, T., Thein, Z.M.M., 2006. Neogene mammalian fauna in Myanmar. Asian Paleoprim. 4, 143–172.

Tantipisanuh, N., Gale, G.A., 2018. Identification of biodiversity hotspot in national level—importance of unpublished data. e00377. Global Ecol. Conserv. 13. <https://doi.org/10.1016/j.gecco.2018.e00377>.

Theobald, W., 1876. Descriptive catalogue of the reptiles of British India. Thacker, Spink and Co., Calcutta.

Thorpe, R.S., 1975. Quantitative handling of characters useful in snake systematics with particular reference to intraspecific variation in the ringed snake *Natrix natrix* (L.). Biol. J. Linn. Soc. 7, 27–43. <https://doi.org/10.1111/j.1095-8312.1975.tb00732.x>.

Uetz, P., Freed, P., Hošek, J., (Eds.), 2019. The Reptile Database. <http://www.reptile-database.org/> (accessed 2 November, 2019).

van Hinsenbergen, D.J.J., Lippert, P.C., Dupont-Nivet, G., McQuarrie, N., Doubrovine, P.V., Spakman, W., Torsvik, T.H., 2012. Greater Indian Basin hypothesis and a two-stage Cenozoic collision between India and Asia. Proc. Natl. Acad. Sci. 109, 7659–7664. <https://doi.org/10.1073/pnas.1117262109>.

Vawter, L., Brown, W.M., 1986. Nuclear and mitochondrial DNA comparisons reveal extreme rate variation in the molecular clock. Science 234, 194–196. <https://doi.org/10.1126/science.3018931>.

Vences, M., Lima, A., Mitalles, A., Glaw, F., 2014. DNA barcoding assessment of genetic variation in two widespread skinks from Madagascar, *Trachylepis elegans* and *T. gravenhorstii* (Squamata: Scincidae). Zootaxa 3755, 477–484. <https://doi.org/10.1164/zootaxa.3755.5.7>.

Vitt, L., Caldwell, J., 2013. Herpetology: An Introductory Biology of Amphibians and Reptiles. Academic Press, London.

Vyas, R., 2001. Notes on the distribution of *Lygosoma lineata* (Gray, 1839) and comments on the systematic status of *L. vosmaerii*. Hamadryad 26, 360–361.

Vyas, R., 2010. Further comments on the systematic status of *Lygosoma vosmaerii* (Gray, 1839). J. Threatened Taxa. 2, 674. <https://doi.org/10.11609/JoTT.o2377.674>.

Vyas, R., 2014. Notes and comments on the distribution of two endemic *Lygosoma* skinks (Squamata: Scincidae: Lygosominae) from India. J. Threatened Taxa. 6, 6726–6732. <https://doi.org/10.11609/JoTT.o3906.6726-32>.

Warren, D., Geneva, A., Lanfear, R., 2017. RWTY (R We There Yet): an R package for examining convergence of Bayesian phylogenetic analyses. Mol. Biol. Evol. 34, 1016–1020. <https://doi.org/10.1093/molbev/msw279>.

Welton, L.J., Siler, C.D., Bennett, D., Diesmos, A., Duya, M.R., Dugay, R., Rico, E.L.B., Van Weerd, M., Brown, R.M., 2010. A spectacular new Philippine monitor lizard reveals a hidden biogeographic boundary and a novel flagship species for conservation. Biol. Lett. 6, 654–658. <https://doi.org/10.1098/rbl.2010.0119>.

Wiens, J.J., Slingluff, J.L., 2001. How lizards turn into snakes: a phylogenetic analysis of body-form evolution in anguid lizards. Evolution 55, 2303–2318. <https://doi.org/10.1111/j.0014-3820.2001.tb00744.x>.

Wu, C.H., Hsu, H.H., Chou, M.D., 2014. Effect of the Arakan Mountains in the north-western Indochina Peninsula on the late May Asian monsoon transition. J. Geophys. Res. Atmos. 10, 769–779. <https://doi.org/10.1002/2014JD022024>.

Wu, C.H., Hsu, H.H., 2016. Role of the Indochina Peninsula narrow mountains in modulating the East Asia-Western North Pacific summer monsoon. J. Clim. 29, 4445–4459. <https://doi.org/10.1175/JCLI-D-15-0594.1>.

Yang, A., 2015. The BPP program for species tree estimation and species delimitation. Curr. Zool. 61, 854–865. <https://doi.org/10.1093/czoolo/61.5.854>.

Yang, Z., Rannala, B., 2010. Bayesian species delimitation using multilocus sequence data. Proc. Natl. Acad. Sci. 107, 9264–9269. <https://doi.org/10.1073/pnas.0913022107>.

Zhang, R., Jiang, D., Zhang, Z., Yu, E., 2015. The impact of regional uplift of the Tibetan Plateau on the Asian monsoon climate. Palaeogeog. Palaeoclim. Palaeoecol. 417, 137–150. <https://doi.org/10.1016/j.palaeo.2014.10.030>.

Zug, G.R., Brown, H.H.K., Schulte II, J.A., Vindum, J.V., 2006. Systematics of the garden lizards, *Calotes versicolor* group (Reptilia, Squamata, Agamidae), in Myanmar: central dry zone populations. Proc. California Acad. Sci. 57, 35–68.